COARSE GRAIN MOBILITY IN A STEP-POOL MOUNTAIN STREAM

by

DUSTIN RANDALL KIMBROW

M.A. LISA DAVIS, COMMITTEE CHAIR

JORDAN A. CLAYTON
JASON C. SENKBEIL

A THESIS

Submitted in partial fulfillment of the requirements
for the degree of Master of Science
in the Department of Geography
in the Graduate School of
The University of Alabama

TUSCALOOSA, ALABAMA

2011

ABSTRACT

Sediment mobility and the resulting erosion of bedrock are the primary controls on surface denudation and landscape evolution in humid subtropical environments. This study investigates the movement of coarse sediment grains in Cheaha Creek, a step-pool headwater stream located in the tectonically passive Talladega Mountains of northeastern Alabama. The frequency and magnitude of stream discharges large enough to mobilize sediment grains ranging from fine sands to large boulders are analyzed in this research. Results indicate that depending on the size and orientation of surrounding sediment grains, coarse gravel to large cobbles are potentially mobile at 1.5 year recurrence interval flows, and the 4.5 - 8.5 year flows have the potential to mobilize small to large boulders. These findings suggest that coarse sediment grains are mobile on relatively short timescales and the opportunity for bedrock erosion and resulting landscape denudation in the Talladega Mountains occurs frequently in the current climatic regime.

LIST OF ABBREVIATIONS AND SYMBOLS

et al.	Latin phrase meaning “and others”
Cfa	Humid subtropical climate as classified by the Köppen Classification System
°*F*	Fahrenheit degrees
mi	Statute mile
km	Kilometer
m	Meter
cm	Centimeter
Ma	Million years
=	Equal to
%	Percentage
n	Manning’s roughness coefficient
Δh	Change in velocity head
τ_o	Mean bed shear stress
τ_c	Critical shear stress
γ_w	Specific weight of water
τ^*_c	Shields Parameter
ρ_s	Grain density
ρ_w	Density of water
g	Gravitational acceleration

ACKNOWLEDGEMENTS

Many thanks are due to God and my great family, for without their encouragement, field assistance, and the strong work ethic they instilled in me, neither this paper nor any of my other endeavors would have ever been completed. I love yall.

CONTENTS

LIST OF TABLES

LIST OF FIGURES

LIST OF EQUATIONS

CHAPTER 1

1.0 INTRODUCTION

This study investigates the movement of coarse sediment grains in Cheaha Creek, a step-pool headwater stream containing both alluvial and bedrock step morphologies in the Talladega Mountains of northeastern Alabama. Step-pool bedforms are dominant features of headwater streams in mountain environments. Because the terrain in which step-pool streams are found is usually rugged and inaccessible, there has been limited research on these bedforms in comparison to alluvial streams (Chin, 1989). However, there has been recent interest in the evolution and fundamental mechanisms of bedrock and mixed alluvial-bedrock streams (Chin and Wohl, 2005). This study seeks to contribute to the growing literature on sediment mobility and step-pool processes in a mixed alluvial-bedrock stream. Previous work on step particle movement in headwater streams has shown that mobility is a function of particle size, discharge, and temporal scale (Chin, 1998). These same factors are analyzed in this research to determine how often step particles are mobilized in the Talladega Mountains of Alabama. This thesis research has several implications including: (1) providing a better understanding of the fluvial history and current processes at work in Cheaha Creek, and possibly for similar step-pool headwater streams in the Talladega Mountains of northeastern Alabama; and (2) testing whether

existing conceptual models of step-pool particle stability (Chin, 1998) adequately explain these processes in different climatic and geologic environments.

1.1 Research Questions

This thesis poses three research questions. First, what are the discharges required to initiate movement of bedform particles in Cheaha Creek? Second, how often do these discharges occur? Third, what implications do the frequency of bedload particle mobility and subsequent step restructuring have for landscape evolution and sediment transport in the Cheaha Creek basin and other similar drainage basins of the Talladega Mountains? Answers to these questions provide further understanding of fluvial processes both modern and relict in the headwaters of Cheaha Creek. The overarching goal of this study is to contribute to the current knowledge on coarse grain sediment transport processes within a post-orogenic, tectonically stable landscape, and the subsequent effects of these processes on landscape evolution in the Talladega Mountains of Alabama.

1.2 Site Description

Cheaha Creek is a second order stream located in the Talladega National Forest in the Talladega Mountains of northeastern Alabama (Figure 1.0). It was selected as a study site because the stream exhibits several step-pool and cascade sequences composed of both alluvium and bedrock. Also, the stream is easily accessed by way of a hiking trail, and the entire study section is located on public U.S. Forest Service (USFS) property.

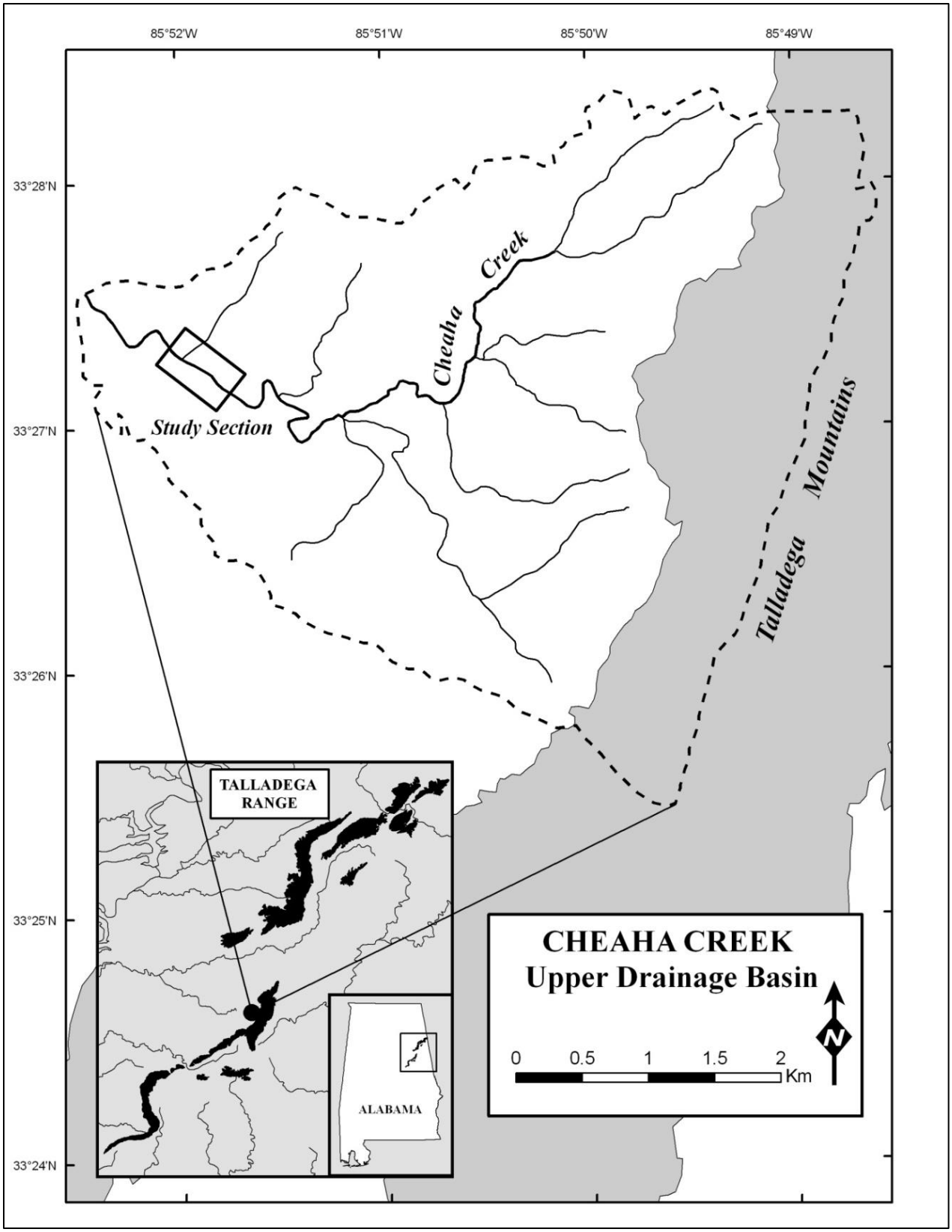

Figure 1.0 Location of the Study section within the Talladega Mountains

1.2.1 Geology

The Talladega Mountains (Figure 1.0) in which Cheaha Creek is located are a SW-NE trending range located in the Northern Piedmont physiographic province of Alabama. The Piedmont Physiographic Province (Figure 1.1) is located in the east-northeast portion of the state and covers approximately 12,845 km^2. The topography of the Piedmont is developed on belts of metamorphic and igneous rocks exhibiting an overall SW-NE trend. Common rock types found in this region are slate, amphibolite, phyllite, quartzite, greenstone, marble, schist, and gneiss (Szabo *et al.*, 1988). The Piedmont is further divided into northern and southern sections by the Brevard Fault Zone (Szabo *et al.*, 1988), with the northern zone exhibiting relatively greater relief due to the differences in erodibility of the underlying strata. The Talladega Mountains, located in the northern zone, mark the southernmost extent of the exposed Appalachian Mountains and contain several of the highest points in Alabama. The Talladega Mountains are the eroded remnants of the geologic terrane known as the Talladega Slate Belt. The Talladega Slate Belt consists of thick sequences of meta-sedimentary and low to medium grade metamorphic rocks that range in age from early Cambrian to middle Paleozoic (Whiting, 2009). Along the study section the stream dissects low grade metamorphic rocks of Silurian to Devonian age known as the Lay Dam Formation (Figure 1.1). The Lay Dam Formation consists of interbedded phyllite, metasiltstone, metagreywacke, metaconglomerate, and quartzite (Szabo *et al.*, 1988). The underlying geologic unit of the extreme upper drainage of Cheaha Creek is a resistant member of the Lay Dam Formation known as the Cheaha Quartzite (Figure 1.1). This stratum forms the majority of the ridge crests in the southern Talladega Mountains.

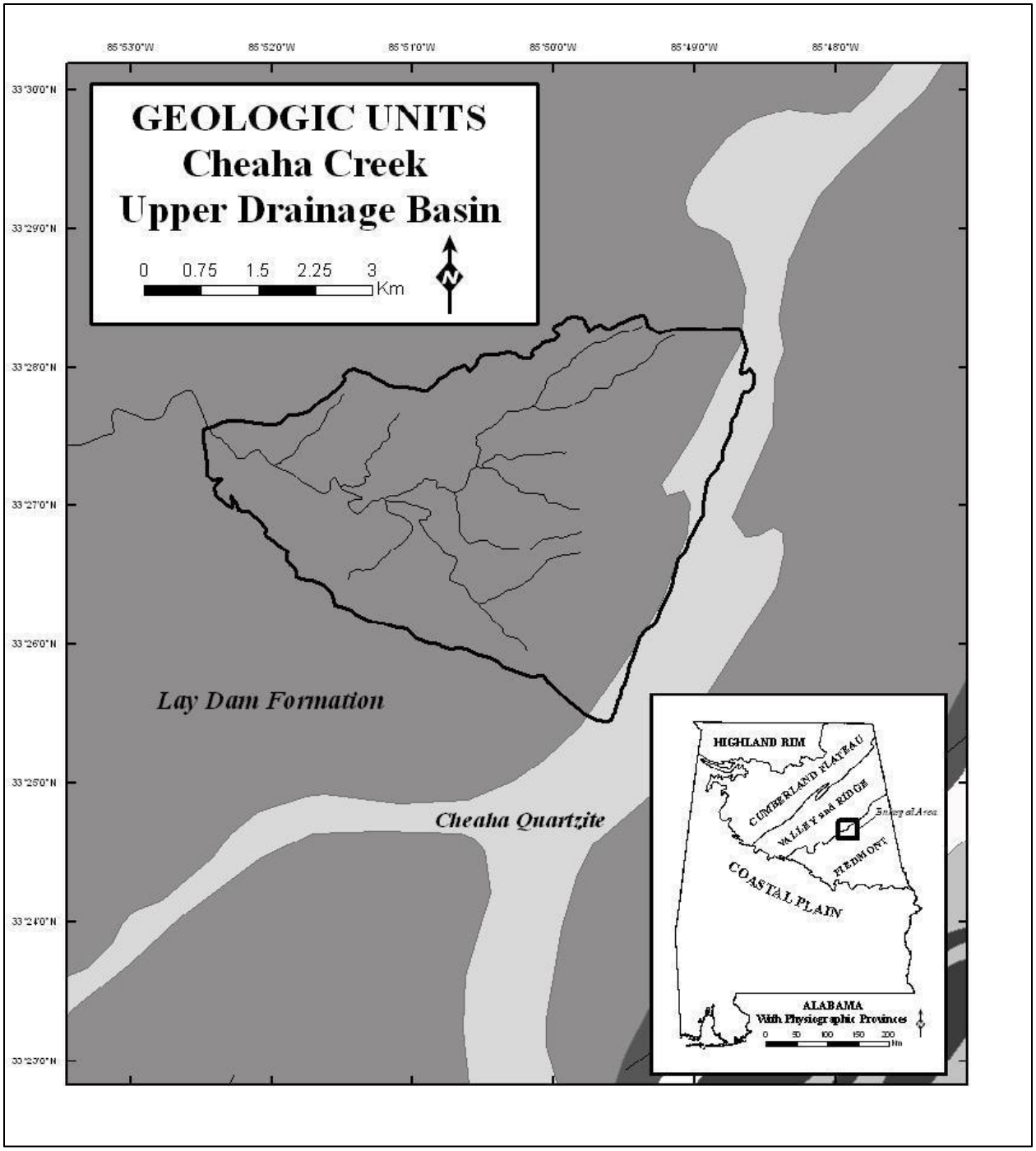

Figure 1.1 Geologic Setting

1.2.2 Geomorphology

Cheaha Creek follows an interesting and varied course within its upper drainage basin, and is divided into the following five distinct sections based on gradient and channel

morphology, beginning upstream: Upper Section, M-bend Section, Study Section, Devil's Den Section, and Lake Chinnabee Section. This thesis research is limited to the Study Section due to time and logistical restraints. The beginning of Cheaha Creek is located at the confluence of two first-order, unnamed streams at approximately 33.462° N, 85.836° W. The 3.0 km section below this confluence is the Upper Section. The Upper Section exhibits a well developed, relatively wide floodplain, with alluvium dominating the channel bed (Figure 1.3). The Upper Section is interrupted near its midpoint by Cheaha Falls, a waterfall with a height of nearly 10 m (Figure 1.4). Below Cheaha Falls the stream resumes its relatively low gradient character and wide floodplain, however bedrock outcrops become more abundant, and alluvium is noticeably coarser. The Upper Section ends as the floodplain narrows and gives way to highly coupled hillslopes, marking the beginning of the M-bend Section. The M-bend Section is approximately 1.0 km long and exhibits higher gradient, more frequent bedrock steps, and less alluvial bed cover compared to the Upper Section. The M-bend Section terminates as the stream exits the narrow valley and resumes a relatively low gradient course referred to in this thesis as the Study Section.

The Study Section (Figure 1.2) is a 380 m section consisting of both step-pool sequences and cascading reaches composed of both alluvium and bedrock. The Study Section has an average slope of 0.014, a narrow floodplain, and at its terminus drains approximately 18.0 km^2. Throughout its upper drainage basin, Cheaha Creek is considered a mixed bedrock-alluvial stream due to the lack of a continuous cover of transportable sediment along both the bed and banks. However, the Study Section exhibits more alluvial character, and the channel is only void of alluvium in areas where bedrock crops out and dips in the upstream direction. The dip angle of these outcrops is large enough to hold back coarse grains, and inherently act as sediment traps.

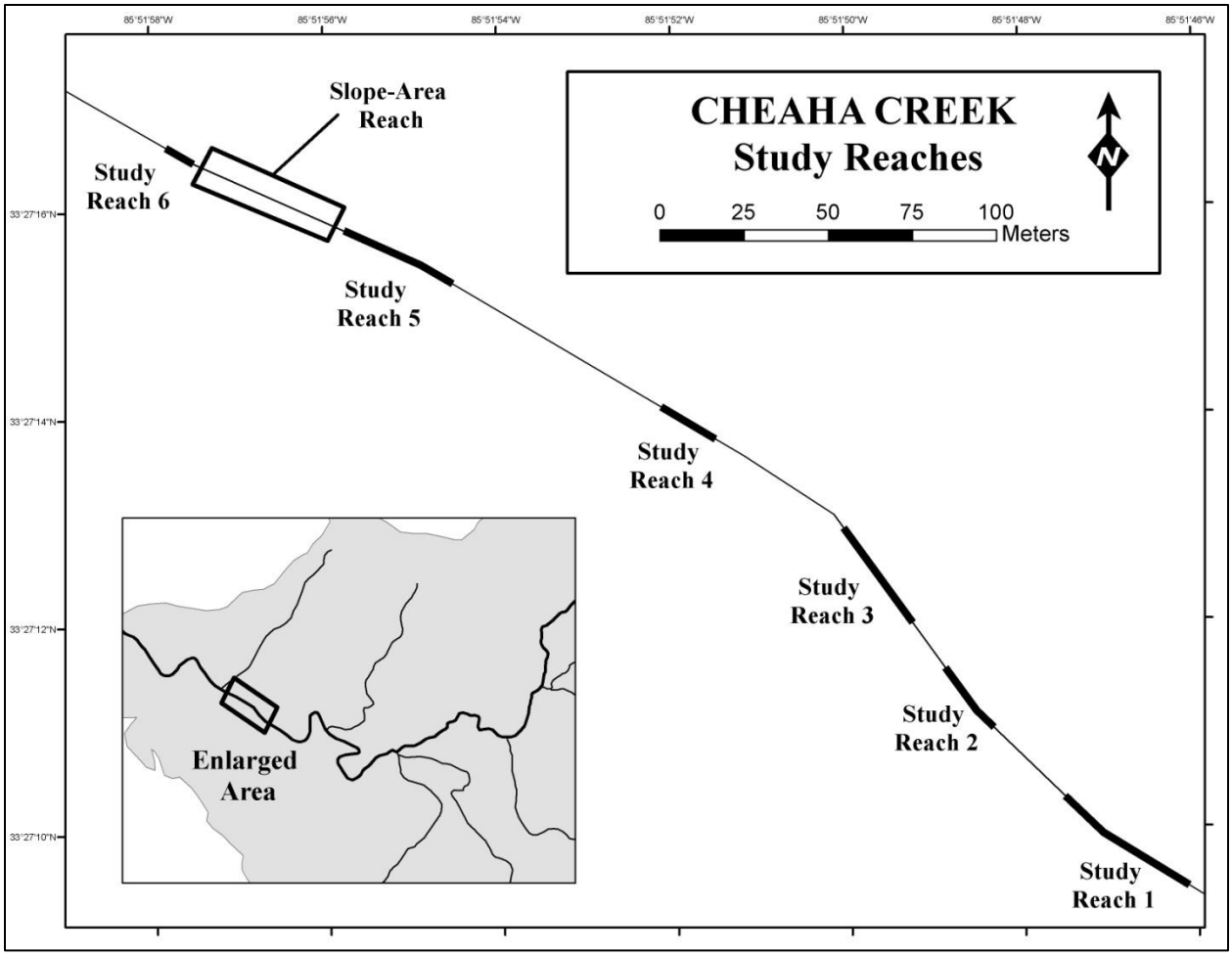

Figure 1.2 Study Reaches

For this thesis research the Study Section was divided into six Study Reaches based on morphologic characteristics, and all data collection and calculations are conducted from these sites. These Study Reaches are named 1 - 6 beginning upstream (e.g. Reach 1, Reach 2, etc…). The Study Section ends at the beginning of a 500 m small gorge section known as the Devil's Den, which is a series of cascading bedrock steps ranging in height from 2-4 m (Figure 1.5). Below the Devil's Den Section is the 600 m Lake Chinnabee Section. This section consists of both step-pool and cascade sequences similar to that of the Study Section and terminates at Lake Chinnabee, an impoundment built by the Civilian Conservation Corps (CCC) in the late 1930's.

Figure 1.3 Cheaha Creek Upper Section

Figure 1.4 Cheaha Falls located in the Upper Section.

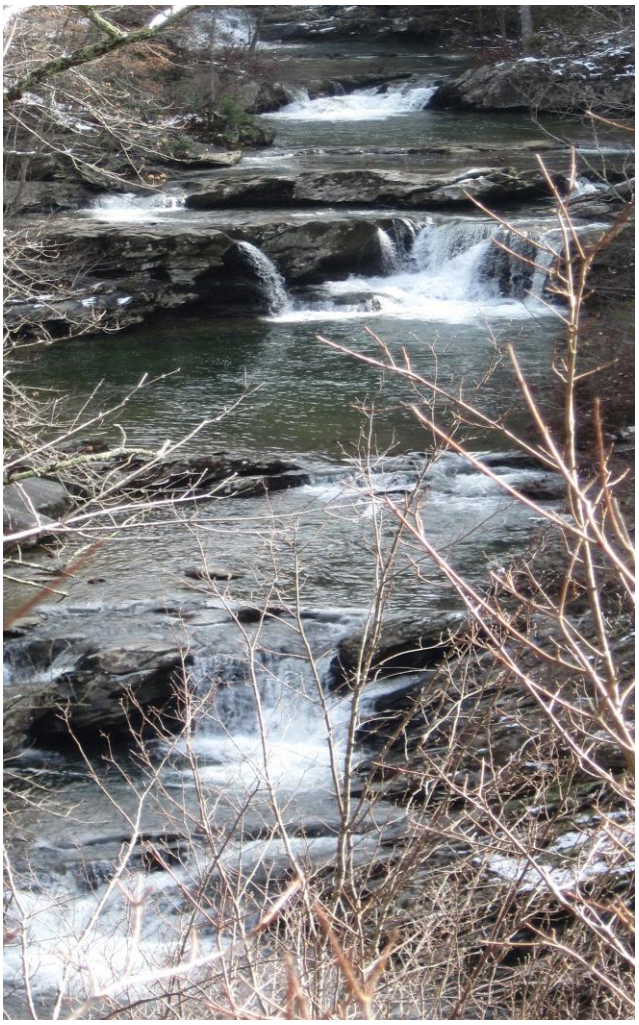

Figure 1.5 Devil's Den Section

1.2.3 Climate

The climate in the Cheaha Creek drainage basin is classified as humid subtropical (Cfa) by the Köppen Climate Classification System (Köppen, 1900). Cfa climate types are characterized by mean temperatures in the coldest month ranging from -3°C to 18°C and above 22°C in the warmest month, with relatively uniform precipitation occurring throughout the year.

The Cheaha Creek drainage basin receives on average 137 cm of precipitation annually (Southeastern Regional Climate Center, 2010). Rainfall is the dominant type of precipitation, and it is distributed throughout the year. The largest rainfall amounts are typically observed in late

winter to early spring. March is historically the wettest month, with mean rainfall totaling 13.15 cm (Southeastern Regional Climate Center, 2010). Cfa climates are typified by humid summers, and the humidity and atmospheric moisture content in the Cheaha Creek drainage basin are due to the close proximity of the Gulf of Mexico. Warm waters in the Gulf of Mexico fuel tropical cyclones that are capable of producing large amounts of precipitation. These storms normally occur from May through October. During mid-summer months the presence of atmospheric moisture coupled with high temperatures typically results in convective storm events. These are localized events capable of producing large amounts of rainfall over short periods of time. Precipitation from autumn to late spring is generally a product of mid-latitude cyclones. These weather systems produce large amounts of precipitation along the frontal boundaries of cold air masses.

Streamflow in the Cheaha Creek drainage basin varies seasonally for a variety of reasons. Due to both the increase in precipitation and the dormancy of vegetation, streamflow is typically greater during the winter and early spring months. If step particles are found to be mobilized under the current hydrologic regime, flow events in Cheaha Creek that may possibly initiate step movement are more likely to occur during these months. Because the Cheaha Creek basin is nearly 100% forested, plant uptake of moisture and resulting evapotranspiration likely limits surface runoff from convective storm events during the summer. However, the duration and intensity of rainfall has been shown to affect surface runoff amounts, regardless of the degree of vegetative cover (Dunne *et al.*, 1991). Therefore, it is possible that long duration storm events associated with summertime and autumn tropical cyclones could also produce particle mobilizing discharges.

1.3 Research Rationale

1.3.1 Current Theories and Findings Regarding Processes and Characteristics in Step-Pool Streams

Step-pool morphology is characterized by an accumulation of large clasts arranged perpendicular to the channel (step) that separates areas of relatively tranquil water containing finer sediment (pool) (Montgomery and Buffington, 1997; Duckson and Duckson, 2001; Chin, 1998, 2003). They typically exhibit a staircase sequence, with a high gradient step leading into a lower gradient pool. Steps and pools are common bedforms in steep mountain streams (Chin, 1999, 2002; Chin and Wohl, 2005; Montgomery and Buffington, 1997), and much literature has focused on the characteristics, organization, and processes associated with these features.

Relationships between geomorphic variables (i.e. step height, pool length, gradient, and wavelength) have been sought by many workers (Grant *et al.*, 1990; Duckson and Duckson, 2001; Chin, 1999; Wohl *et al.*, 1997; Wohl and Grodek, 1994). Chin (1999) investigated the morphologic characteristics of step height and wavelength in headwater streams of the Santa Monica Mountains of southern California. She also explored the processes and relationships producing the observed characteristics. Chin (1999) defined step wavelength to be the linear distance between successive pools, and step height as the perpendicular distance between the top of a step and a hypothetical line connecting successive pool troughs. Her study found a positive correlation with step morphologic structure (height, wavelength) and gradient. However, Chin argued that the size of step forming rocks, rather than gradient, is the primary control of the height of steps; and wavelength is a function of step forming discharges. Chin's study contributed to the theoretical understanding of step-pool morphology, particularly step height, and its results confirm what others (Wohl *et al.*, 1997) have suggested, namely that step height is

controlled by particle size. Duckson and Duckson (2001) investigated relationships between step pool variables (pool length, step height, pool depth) in a high gradient stream in the Oregon Cascades exhibiting both alluvial and bedrock steps. Their study stream flowed over three different types of igneous rock, and differences in geomorphic form over the varying lithologies were examined. Results of this study indicated no significant relationship between pool length or pool depth to slope in any rock type. Step height was positively correlated with slope in andesite and basalt, and a weak correlation was found in dacite. The authors noted that due to scatter and inconsistent trends in the data, neither pool length, depth, nor step height provided useful information when independently compared to slope. However, when slope is compared to a ratio of step height to pool length, there is a significant correlation in each rock type. These results indicated that regardless of differences in lithology, steeper slopes produced smaller pool lengths. Duckson and Duckson (2001) also implied that despite variation of rock type, steps and pools adjusted their form to dissipate energy most efficiently. Wohl and Grodek (1994) studied the relationships between channel bed step characteristics in an ephemeral stream containing both bedrock and alluvial steps in Israel. They found a strong correlation between the height and spacing of bed steps and channel slope. Step height was found to increase with gradient. Results also showed that there was no significant difference in length between alluvial or bedrock pools if slope is greater than 20%.

Chin (2002) studied the wavelengths of step pool bedforms in selected reaches of the Santa Monica Mountains of southern California in an effort to determine if the period or length between these bedforms follows a regular pattern, even when influenced by external factors such as vegetation and boulders. She found that although external factors such as bedrock, debris, and vegetation do affect the periodicity of step pool bedforms, the regularity in which these bedforms

are organized was not entirely eliminated. Chin argued that the resilience of step pool periodicity suggested the presence of general internal mechanisms that work toward equilibrium between discharge, sediment, channel morphology, and energy expenditure. She suggested a connection between internal mechanisms, channel morphology, and energy expenditure by referring to the theory that step pool streams meander in the vertical dimension (i.e. channel bed undulations). Several other researchers (Keller and Melhorn, 1978; Richards, 1976) also suggested that because step-pool streams are typically horizontally confined by bedrock walls or valley hillslopes, the undulating nature of steps and pools may be likened to meandering in the vertical dimension.

Chin (2003) also investigated the potential for steps to dissipate energy at different discharges. At low flows, steps are independent variables effective at controlling flow direction, and reducing potential energy. In the Santa Monica Mountains of southern California steps accounted for 80-100% of elevation (potential energy) losses (Chin, 2003). This energy decrease counteracts the steep gradients of headwater streams, thus reducing erosive potential. At higher flows where steps become submerged, the energy dissipation effect diminishes. Steps then become dependent variables, adjusting to flow variations, and behaving more as channel bed roughness elements (Chin, 2003; Bathurst, 1987) analogous to riffles. Because the height of a step will determine the frequency of its submergence, it can be inferred that over time, larger steps will function more frequently as energy dissipaters. Smaller steps, being submerged more frequently, function as bed roughness elements a larger part of the time.

Chin (1998) analyzed the stability of steps in the Santa Monica Mountains of southern California and found that steps may undergo reorganization from 5 to 100 years, depending upon the average size of the five largest clasts in a step. Chin recognized that understanding the

timescales at which the step-pools are destabilized and reorganized promotes better understanding of bedrock streams, as well as a more complete perception of landscape evolution. Chin found that channel steps may be considered stable and unstable, depending on the temporal scale. As the length of time increases, the likelihood of instability also increases. Instability may be exacerbated if the most frequently occurring largest clasts within a step are relatively small and thus more mobile (Jackson and Beschta, 1982; Chin, 1998). Because steps are typically composed of an accumulation of heterogeneous particle sizes, the larger grains have a tendency to hide smaller particles and prevent their entrainment during flows that would otherwise initiate motion. Therefore, the coarse material must first become mobile in order for the step as a whole to become entrained (Chin, 1998; Andrews, 1983; Parker and Klingeman, 1982).

Keller and Melhorn (1978) found no significant difference between the average spacing of 251 pools for both alluvial and bedrock streams. The length of spacing for both types was also found to be normally distributed in pool and riffle morphology streams, which is similar to step-pool morphology. They concluded from these data that pool and riffle development was a fundamental feature of many streams. They proposed that thalweg elevation undulations, whether in horizontally confined or fully developed meandering streams, are evidence for a natural form of energy dissipation. Wohl *et al.* (1997) studied the function and characteristics of log and clast steps in headwater step-pool streams in northwestern Montana. Results from their study indicated that step spacing is proportional to channel slope, bankfull width, and drainage area. They also found a positive correlation with step height and channel width. There was no significant difference between the height or spacing of clast steps and log steps, and they suggested that the locations of clast steps are dependent upon the placement of relatively immobile woody debris jams.

Gomi *et al.* (2003) studied the effects of timber harvesting and mass movement on the distribution of steps in headwater streams of Alaska. They found that recruitment of woody debris into streams subsequent to logging activities altered sediment transport and led to channel obstructions. They also found that localized mass movements altered the structure and morphology of steps. This study provided quantitative evidence that headwater streams are capable of adjusting their morphology to external inputs, both colluvial and biologic.

Step-pool morphology has previously been explained by analysis of relationships between geomorphic variables (i.e. step height and length, pool height and length, pool depth, slope, step particle size, wavelength, and drainage area). The literature has shown that relationships between these variables indicate that step-pool morphology develops to increase flow resistance in a high energy environment (Abrahams *et al.*1995; Chin and Wohl 2005). Stepped-bed morphology is likened to meandering in the third (vertical) dimension by many researchers (Richards, 1976; Keller and Melhorn, 1978; Chin, 2002) as a form of energy expenditure. This theory was further substantiated by the work of Wohl *et al.* (1997), Duckson and Duckson (2001), and Gomi *et al.* (2003) where variability in the types of steps (e.g. log, bedrock, alluvial) did not influence the spacing of steps. Chin (2003) suggested that although the step-pool sequence acts as an independent variable and immobile energy dissipater at low discharges, high flows entrain the step framework particles. They then become dependent variables, responding to discharge and sediment variations. Chin (1998) investigated the timescales at which steps are restructured. Although her work provided valuable information regarding step-pool mobility, it was limited to a single location in southern California. Chin and Wohl (2005) recognized the need for further work on the formation and movement of steps in a range of environments.

1.3.2 Significance of Bedrock and Mixed Bedrock-Alluvial Streams in Landscape Evolution Studies

Montgomery and Gran (2001) stated that recently there has been a rise of academic interest in the processes of fluvial bedrock incision and its relationships to landscape evolution. They attributed this increased interest to the fact that many of the paradigms in fluvial geomorphology are based upon the processes occurring within alluvial river systems (Leopold *et al.*, 1964), rather than bedrock and mixed bedrock-alluvial systems such as Cheaha Creek. Whipple and Tucker (2002) suggested that bedrock channels determine the relief and topography of mountain landscapes, especially those not influenced by glaciation, and therefore are essential in furthering the understanding of landscape evolution. Whipple and Tucker (2002) defined landscapes in which there is a state of equilibrium between tectonic uplift and erosion as "steady-state" topography. Within bedrock and mixed bedrock-alluvial streams, such as Cheaha Creek, there are primarily two end-member categories with respect to landscape denudation via erosional processes - streams with sediment supply exceeding sediment transport ability (transport limited), and streams with transport ability exceeding sediment supply (supply limited) (Whipple and Tucker, 2002). This variation between supply and competence has an effect on the bed characteristics, and thus the channel morphology of a particular stream or reach. According to Skylar and Dietrich (2006), the presence of sediment within a bedrock stream will produce essentially two different scenarios. In a transport limited system, sediment on the streambed will abrade the bed and induce erosion as discharge increases and critical shear stress thresholds for particle entrainment are reached. However, if there is too much sediment present, the bed will be covered and erosion will not take place. If the stream exhibits supply limited characteristics, the

channel bed will be nearly void of sediment, due to the constant ability for the stream to transport the supplied sediment. In these supply limited channels, erosion occurs primarily from the detachment of bedrock. The channel morphology of bedrock streams is therefore dependent on stream competence, capacity, and sediment supply.

Jansen (2006) investigated fluvial incision rates in a post-orogenic, arid landscape of southeastern Australia. He stated that the majority of previous research on fluvial incision had been limited to tectonically active environments (Whipple and Tucker, 1999; Tomkin *et al.*, 2003) and fluvial denudation research in passive geologic cratons was needed. Jansen calculated paleoflood discharges using a step-backwater model and developed mean bed and critical shear stress values for particle entrainment. Mean bed shear stress values ranged from 37 - 517 N/m^2 for a discharge of 350 m^3/sec. Jansen termed this discharge the "formative" flow due to its ability to mobilize the D_{84} grain size class. His work found relatively slow fluvial incision rates into bedrock at < 5m/Ma.

1.3.3 Ecological Importance of Step-Pool Bedforms and Large Woody Debris

Step-pool bedforms in forested mountain streams are often composed of accumulations of large woody debris (LWD) (Marston, 1982). LWD has been shown to be an integral part of the fluvial system, both as an agent for geomorphic work and for improved ecological habitat (Gregory and Davis, 1992; Abbe and Montgomery, 1996; Bisson *et al.*, 1987; Wallace *et al.*, 1995). LWD can be recruited into a stream by two general delivery methods: chronic delivery and episodic delivery (Bisson *et al.*, 1987). Chronic delivery is characterized as normal tree mortality or gradual bank erosion, alternatively, episodic delivery is normally viewed as an event of large magnitude and less frequency (e.g. landslides). In forested mountain streams, LWD is

often a primary factor in determining channel morphology, forming pools and waterfalls, influencing storage and transport of sediments, gravels, organic matter, and nutrients (Bisson *et al.* 1987). Sedell *et al.* (1988) reported that LWD promoted the retention of sediments, organic matter, and nutrients which in turn influences and enhances successional abilities of riparian vegetation by providing new surfaces for their establishment. LWD can also function as 'nurse logs' that facilitate new growth (Franklin, 1982; Harmon *et al.*, 1986).

Pools are considered to be important for energy reduction and facilitating sediment storage, as well as providing aquatic habitat (Dolloff, 1986). Bilby and Likens (1980) found that coarse particulate organic matter (CPOM) such as leaves were retained within a stream system for a longer time as a result of LWD dams. CPOM eventually decomposes, producing fine particulate organic matter (FPOM) and therefore improving the vigor of the local aquatic community.

1.3.4 Summary

In summary, the current state of research conducted in step-pool systems is lacking in several areas, including direct observations and empirical data of discharge and sediment transport at the upper range of flows, relationships between mixed bedrock-alluvial streambed topography and water surface profiles across the upper range of discharges, and coarse grain sediment mobility in post-orogenic landscapes. This thesis addresses the gaps in post-orogenic sediment processes, and provides useful data on the mobility of coarse grains in these environments.

CHAPTER 2

2.0 METHODS

2.1 Introduction

This study endeavors to answer two specific research questions regarding coarse sediment grain mobility, and use the information gained to improve theories of landscape evolution. First, what are the discharges required to initiate movement of bedform particles in Cheaha Creek? Second, how often do these discharges occur? In order for entire steps to be moved downstream, streamflow discharges large enough to initiate entrainment of the largest clasts that structure the framework of an individual step must occur (Chin, 1998; Costa, 1983). High magnitude discharges, which are theoretically the type of flows required to restructure steps, are infrequent, short lived, and difficult to observe in the Cheaha Creek drainage basin. Thus, for this thesis research hydraulic flow equations are used to mathematically estimate the threshold discharges required to initiate sediment grain movement. This study utilizes two techniques for mathematically estimating the threshold discharges required for coarse grain movement, and results from both methods are compared. The Costa Method is discussed first and is based on the theory that stream competence is a function of velocity. This technique involves calculating both critical discharge and the sediment grain size mobilized by the flow. The second method determines critical shear stress for sediment grains by utilizing an adjusted form of the Shields Equation. The Slope-Area Equation is used to indirectly calculate discharge, which is necessary to relate the calculated critical shear stress for movement of sediment grains

to a discharge value. These computations and data collection are performed for six Study Reaches exhibiting independent and distinct morphology which are located within the 380 m Study Section.

2.2 Field Data Collection

Similar field parameters are required for the Costa Method, Shields Method, and the Slope-Area Equation employed in this thesis research at six study reaches. Bed slope, channel/valley cross-sections, and particle size data were collected at each study reach. Two separate cross-sections meeting the requirements set forth in Dalrymple and Benson (1967) were also surveyed for use in the slope-area discharge calculation. Cross-sections were surveyed by stretching a tagline across the entire valley at the beginning of each reach and noting the depth with a leveling rod at both 0.5 m intervals and important changes in topography. The channel bed slope was surveyed with a Sokkia Laser Level and leveling rod at points along the entire Study section. All bed slope and cross-section survey points were then tied to an arbitrary vertical datum.

Particle size data were collected at each of the six study reaches following the methods of Zimmerman and Church (2001), where sediment grain sampling is conducted using two different techniques. First, fine sediment was bulk sampled from distinctive deposits. This material is typically deposited behind large bedrock outcrops or large boulders and along the channel margins. Because these deposits are considered distinct and visibly different in character than the overall grain size distribution of the stream, a separate particle size distribution of the *b-axis* diameter was conducted from this population (Zimmerman and Church, 2001). Second, a pebble count (Wolman, 1954) of ~100 grains of gravel to boulder size (4 to >256 mm) particles was

conducted along transects perpendicular to the flow at each study reach, and the three principal axes of each particle was measured using a folding ruler, which typically encompassed 25-75% of the visible boulders within each study reach. All three principal axes (a,b,c) were measured in order to both minimize error and to compare shear stress values for each diameter axis. This method is conducted due to the relatively flat nature of the coarse grains in Cheaha Creek. The shear stress equations utilized in this research rely on the *b-axis* alone to determine critical stresses. However, due to the flatness of many sediment grains as well as their imbricated position on the streambed, even for relatively large clasts the *b-axis* length does not always protrude through the laminar sub-layer and into the turbulent layer in order for drag and fluid forces to be most effectively applied. Because of these factors, all three principal axes are measured and shear stress determined for different grain size classes.

The gravel-boulder sampling was then compiled into separate grain size distributions for each axis. This coarse grain sample characterized the dominant population of sediment in the study reaches of Cheaha Creek. Bedrock outcrops within the channel of Cheaha Creek are oriented in the same direction as the imbricated alluvial particles, so care was taken not to mistakenly count a bedrock outcrop as a large boulder. Large colluvial boulders were excluded from sampling, but their location and orientation was noted. Boulders were determined to be colluvial based on their outlying size and lack of imbrication. The D_{50}, D_{84}, and D_{90} particle size percentiles of each principal axis were calculated from these data for the adjusted Shields critical shear stress calculations.

2.3 Hydraulic Equations

2.3.1 The Costa Method

Previous workers (Hjulstrom, 1935; Bradley and Mears, 1980; Costa, 1983; Thorne and Zevenberger, 1986; Chin, 1998) have utilized velocity to model stream competence. Their methods followed the principle that particle size is proportional to some measure of velocity (Hjulstrom, 1935; Leliavsky, 1955). Costa (1983) utilized this method to recreate paleoflood discharges from boulder deposits for steep mountain streams in the Colorado Front Range, and Chin (1998) modeled the stability of steps in the Santa Monica Mountains of California. This thesis employs the method developed by Costa (1983) and later utilized by Chin (1998) that combines velocity equations (two theoretical and two empirical) by means of arithmetic averaging to model stream competence. Chin (1998) and Costa (1983) both argued that averaging these four equations may provide the most accurate results because no single velocity equation has yet shown to be superior in modeling coarse and heterogeneous particle movement.

The Costa Method combines three equations to derive a competent particle size and compute discharge. First, Costa's original equation to derive mean depth from particle size (Costa, 1983) is modified to compute a competent particle size from field measurements of mean depth (Equation 2.1). Second, the Continuity Equation (Equation 2.2) is used to compute discharge, however, the velocity term in the Continuity Equation must first be determined by using Costa's Velocity Equation (Equation 2.3) which utilizes particle size as the independent variable to calculate velocity.

Depth equations utilized by Chin (1998) and Costa (1983) were constructed using an average of the following four methods: an adjusted form of Manning's roughness coefficient equation, an empirical curve relating coarse particles and unit stream power for mobility, an

abridged form of the Shields' Equation (Shields 1936), and a relative smoothness equation. Each of these equations is explained further in Table 2 of Costa (1983). These equations use an average of the five largest clast sizes as the independent variable to derive mean depth, and the depth equations for different slopes are plotted in Figure 2.1 (modified from Costa, 1983). The Study Section has an average bed slope of 0.014, thus the equation used for this thesis is interpolated between Costa's depth curves. Because Costa was recreating paleoflood channel

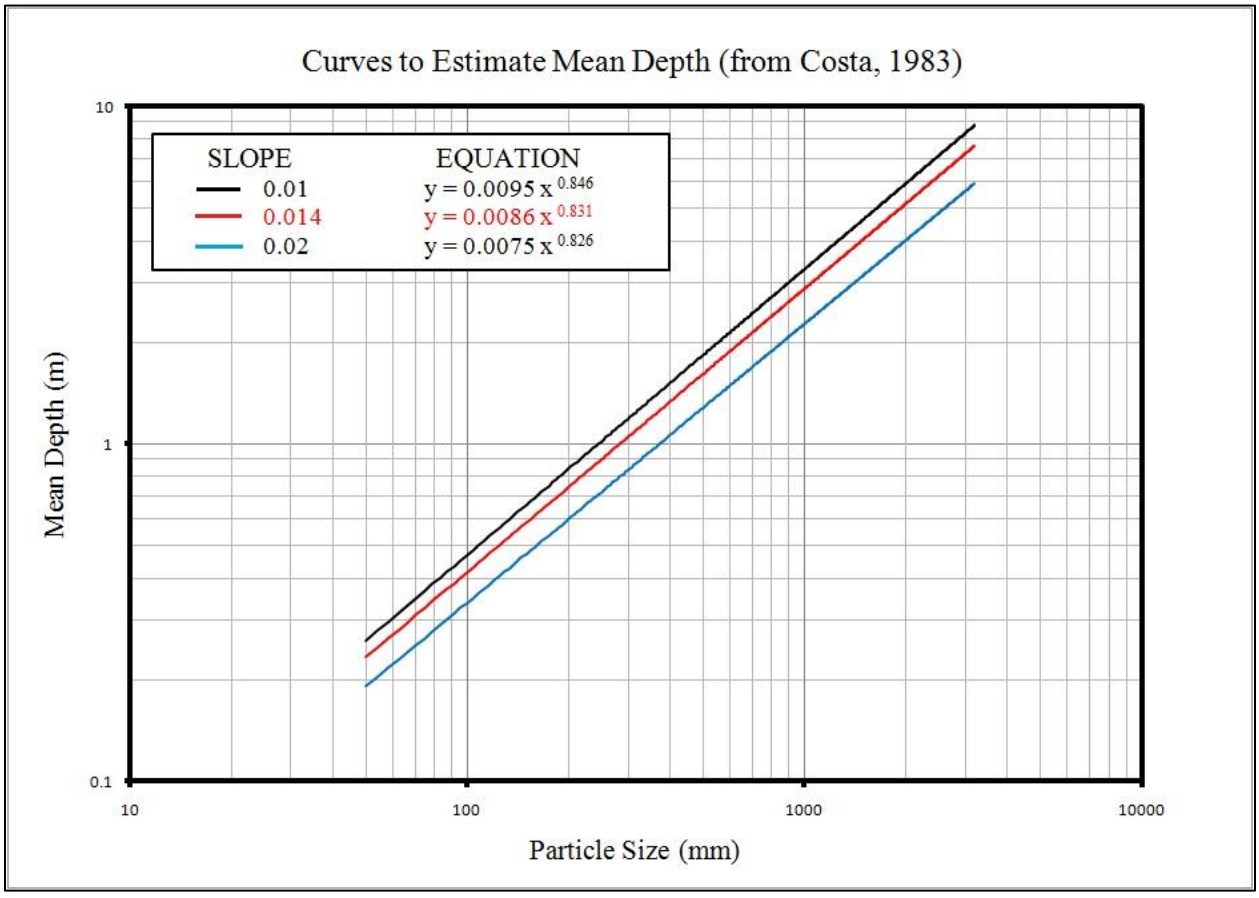

Figure 2.1 Curves for estimating mean depth (from Costa, 1983).

The red line is the interpolated curve used for this thesis (average slope of 0.014)

Where y = mean depth (m) and x = particle size (mm)

conditions and could not actually collect the data in the field, he needed to mathematically compute the mean depth of flow. However, for this thesis research mean depth is determined from field measurements, so the interpolated equation for slope of 0.014 (Study Section average slope, $y = 0.0086x^{0.831}$, Figure 2.1) to derive mean depth from particle size was rearranged to solve for particle size using mean depth as the independent variable (Equation 2.1). Mean depth values at 6 different water surface elevations above an arbitrary vertical datum at each study reach are then entered into Equation 2.1 to determine the competent particle size for each water surface elevation.

Equation 2.1

Equation to Derive Particle Size from Mean Depth (Slope = 0.014)

$$d = 306.73\ D^{1.2}$$

D = mean depth

d = particle diameter *b-axis* (mm)

Discharge is computed using the Continuity Equation (Equation 2.2). This equation is based on the Law of Conservation of Mass (Darcy's Law), and when applied to hydraulics states that a quantity or mass of flow that passes through a given area cannot be created or destroyed. This allows for the assumption that the volume of flow will remain constant between two points or cross-sections provided there is a negligible amount of inflow from surface runoff or outflow/inflow through groundwater interactions. Discharge is then calculated by simply multiplying the cross-sectional area of the channel, which is derived from field measurements, by the downstream velocity of water.

Equation 2.2

Continuity Equation to Calculate Discharge

$$Q = A\ V$$

Q = discharge (m^3/s)

A = cross sectional area (m^2)

V = velocity (m/s)

Costa (1983) used an average of the five largest clast sizes as the independent variable to derive average velocity at each step. The five largest clasts in each step were used because although steps are generally composed of an accumulation of heterogeneous particle sizes, the clasts that form the step framework typically range from cobble to boulder size. These larger particles act to shield the smaller grains from entrainment, and therefore restrict the mobilization of entire steps to discharges that are able to entrain the larger, framework particles (Chin, 1998; Andrews, 1983; Parker and Klingeman, 1982). Costa (1983) provided detailed descriptions of all computations used to develop the working equations used in this thesis. Below is Costa's final equation for modeling mean velocity.

Equation 2.3

Mean Velocity

$$V = 0.18d^{0.487}$$

V = mean velocity (m/s)

d = particle size (mm)

2.3.2 The adjusted Shields Equation for critical shear stress calculations

This thesis research also utilizes basic principles and equations of tractive force to determine the threshold discharges required to initiate motion of sediment grains in Cheaha Creek. The mean bed shear stress (Equation 2.4) and critical shear stress (Equation 2.5) to initiate motion of grain size populations are computed for 6 water surface elevations at each study reach. The ratio of mean bed shear stress to critical shear stress (τ_o / τ_c) is then used to provide a measure of the entrainment potential. Where $\tau_o / \tau_c = 1$ (mean bed shear stress value was equal to computed critical shear stress value per grain size), it is assumed for the purposes of this thesis research that incipient motion of the particular grain size in question occurred.

Much research has been conducted regarding initial motion of sediments from tractive force (Shields, 1936; Miller *et al*., 1977; Wiberg and Smith, 1987; Komar, 1987; Buffington and Montgomery, 1997). A sediment grain resting on the surface of the channel bed will begin to move when the driving forces acting on the particle overcome the resisting forces keeping it in place. Resisting forces acting on a particle are the particle's effective weight (gravity minus lift and buoyancy) and its angle of repose, which is a measure of the difficulty of the grain moving out of its position with respect to the surrounding particles (Wiberg and Smith, 1987). The angle of repose, also known as the friction angle or pocket geometry, depends on the arrangement and sorting of the surrounding particles. Driving forces acting on a sediment grain are gravity, buoyancy, lift, and drag. Lift and drag are forces that result from fluid flow on and around the particle. A measure of drag force exerted per area on a particle that is resting on the channel bed at a particular depth of flow is the bed shear stress (τ_o), and is defined by Equation 2.4.

Equation 2.4

Mean Bed Shear Stress

$$\tau_o = \gamma_w R S$$

τ_o = mean bed shear stress (N/m^2)

γ_w = specific weight of water (N/m^3)

R = hydraulic radius (m)

S = water surface slope

For this thesis research, mean bed shear stress values are calculated for each of the six study reaches as well as for the cross-sections used in the slope-area discharge calculations. The specific weight of water for these shear stress calculations is assumed to remain constant at 9810 N/m^3. Hydraulic radius and water surface slope are variables required from field data for the Mean Bed Shear Stress Equation (Equation 2.4). Hydraulic radius is defined as the ratio of the channel cross-sectional area to wetted perimeter, and will vary depending on both discharge and the channel geometry at a particular cross-section. For this research, hydraulic radius is computed from cross-sectional geometry at each of the six study reaches at 6 different water surface elevations using WSPRO software. The water surface slope in the study section of Cheaha Creek was gathered from a field survey of the channel bed, and is assumed to be parallel to the overall channel bed slope of the Study Section. The true slope of the water surface will vary at different stages, but without visual observation of floods or reliable high water marks the actual slope for a given discharge is difficult to determine.

The equation for computing critical shear stress (Equation 2.5) for a sediment grain was developed by A. F. Shields (1936) from laboratory flume data of near-uniform grain sizes to determine threshold stress values for incipient motion of particles from tractive force under flow

Equation 2.5

Shields Parameter Equation

$$\tau^*_c = \tau_c / (\rho_s - \rho_w)\, g\, D$$

τ_c = critical mean bed shear stress (N/m^2)

τ^*_c = Shields Parameter

ρ_s = grain density (2650 kg/m^3)

ρ_w = density of water (1000 kg/m^3)

g = gravitational acceleration (9.81 m/sec^2)

D = diameter of grain *b-axis* (m)

of water (Buffington, 1999). A particle's resistance to shear stress is determined by its size and position relative to the surrounding particles, as well as the hydraulic roughness of the flow (Wiberg and Smith, 1987; Komar, 1987). This resistance to stress is expressed in Equation 2.5 as a nondimensional coefficient known as the Shields Parameter (τ^*_c). This coefficient is an important factor in determining the threshold amount of shear stress required for incipient motion of a sediment particle under flow of water. Shields argued that this nondimensional parameter was related to the boundary Reynolds Number for homogeneous grains, and reached a nearly constant value of 0.06 for flow with a boundary Reynolds Number (Re^*_c) near 500

(Buffington and Montgomery, 1997). The boundary Reynolds number is a measure of turbulence at the channel bed, and flow is considered turbulent when $Re \geq 2000$.

Most mountain streams such as Cheaha Creek contain a range of particle sizes. Poorly sorted beds, especially with a large range of grain sizes and a highly irregular bed surface, introduce variables such as particle hiding and protrusion that are not accounted for in the original Shields Parameter. To account for this heterogeneity, calculations of critical shear stress in channels with poorly sorted bed sediments must utilize either an adjusted value for the Shields Parameter or an adjusted form of the original Shields Parameter Equation (Equation 2.5) (Wiberg and Smith, 1987; Komar, 1987; Buffington and Montgomery, 1997). Because Cheaha Creek exhibits a large range of grain sizes as well as a highly irregular bed surface, this thesis research utilized an equation developed by Komar (1987) to compute critical shear stress for various grain diameters (Equation 2.6). There are many variations of the original Shields Parameter Equation for critical shear stress (Buffington and Montgomery, 1999), and Equation 2.6 is used for this thesis research because of its applicability to streams with poorly sorted grains of gravel size and

Equation 2.6

Dimensional Critical Shear Stress

$$\tau_c = 0.045\ (\rho_s - \rho_w)\ g\ D_{50}^{0.6}\ D_i^{0.4}$$

τ_c = critical mean bed shear stress (N/m^2)

ρ_s = grain density (2650 kg/m^3)

ρ_w = density of water (1000 kg/m^3)

g = gravitational acceleration (9.81 m/sec^2)

D_{50} = diameter of the median grain axis (m)

D_i = diameter of the grain of interest axis (m)

larger (Jansen, 2006). Jansen (2006) utilized this equation for a similar study in a mixed bedrock-alluvial stream of comparable size and sediment heterogeneity. This equation relies on the theory that a sediment grain's resistance to motion depends on its position and size relative to the position and size of the surrounding particles. Critical shear stress is computed with regard to the ratio of the particle size of interest to the median diameter particle within each reach (D_i/D_{50}). For this thesis research critical shear stress is calculated for the following grain diameters of each principal axis within each reach: D_{50}, D_{84}, and D_{90} for both the coarse grain population and the distinct fine grain deposits, and the average diameter of the 5 largest particles in each reach. Komar (1987) suggested that this equation remains applicable even for larger outlying grains as long as the D_i clasts are unmistakably part of the prevailing grain size distribution. This equation does not however account for the degree of imbrication and the distance a grain protrudes into the flow.

2.3.3 Slope-Area Equation for calculating discharge

Discharge is required for this thesis to determine how often coarse grain sediments are transported downstream. Because Cheaha Creek is an ungaged site, indirect methods for calculating discharge must be employed. There are several methods for indirectly calculating discharge in open channels, and for this thesis research the Slope-Area Equation is used. The Slope-Area Equation for calculating discharge utilizes an equation based on steady uniform flow (i.e. the water surface profile and energy gradient are parallel to the streambed, the area and depth of flow remains constant throughout the reach, and flow is constant in both time and space) that requires channel geometry characteristics, Manning's roughness values (Manning's

n), and energy gradient (Dalrymple and Benson, 1967). Conditions of steady uniform flow are rarely seen in natural channels, but Dalrymple and Benson (1967) give the following guidelines for selecting an ideal reach and cross-sections for application of the Slope-Area Equation:

1. the channel shape should be uniform between cross-sections as well as above and below the slope-area reach;
2. a straight reach is preferred;
3. a contracting reach is more desirable than an expanding reach;
4. the fall in the reach should be equal to or greater than 0.5 ft (0.15 m);
5. the length of the reach should be greater than or equal to 75 times the mean depth of the channel;
6. subcritical flow conditions (Froude < 1);
7. the surveyed cross-sections should be characteristic of the entire reach;
8. all flow in the channel should be perpendicular to cross-sections (effective flow).

A channel reach with these characteristics is assumed to exhibit gradually varied flow, which is acceptable for slope-area calculations. The Slope-Area Equation combines the Continuity Equation (Equation 2.3), the Manning Equation (Equation 2.7), and the Energy Equation (Equation 2.8) to derive the Final Slope-Area Equation (Equation 2.11) for discharge calculations.

The Manning Equation (Equation 2.7) is the basis for the Slope-Area Equation and computes discharge from channel characteristics (i.e. cross-sectional area, wetted perimeter, and hydraulic radius), Manning's Roughness Coefficient, and the energy gradient or slope between

Equation 2.7

Manning Equation

$$Q = (1/n)\ A\ R^{2/3}\ S^{1/2}$$

Q = discharge

n = Manning's roughness coefficient

A = cross-sectional area

R = hydraulic radius

S = energy slope

cross-sections. Cross-sectional area is defined as the wetted area below the water surface at a cross-section perpendicular to the flow, the wetted perimeter is the linear perimeter of a cross-section's wetted boundary surface, and hydraulic radius is the ratio of cross-sectional area to wetted perimeter (A/P_w). These channel characteristics are derived from cross-section data surveyed in the field.

The Manning's Roughness Coefficient (Manning's *n*) is used to quantify the friction loss exhibited by flow over different surfaces (Barnes, 1967). Because natural channels vary greatly in characteristic and form, there is no set value of Manning's *n* for a particular channel size or type (Barnes, 1967). However, there are several methods for determining Manning's roughness coefficient, and this thesis research employs a technique developed by Cowen (1956). The Cowen method is an additive technique where a base *n* value is selected depending on bed material characteristics, and values are then added and multiplied to account for other channel irregularities. Additive values for the Cowen method are taken from a table in Arcement and Schneider (1989). Equation 2.8 shows the formula for the Cowen method for estimating

Manning's roughness coefficient. For this thesis, Manning's roughness values are computed for three subsections of each cross-section of channel based on the Cowen technique. The left and right overbank subsections were given roughness values of $n = 0.124$, primarily due to both dense vegetation and surface obstructions such as bedrock outcrops and colluvial boulders. Bed material size and bedrock outcrops result in the computed channel subsection roughness of $n = 0.075$. Table 2.1 below shows the computation of Manning's n using the Cowen method. Figure 2.2 show the location of breaks in roughness along both slope-area cross-sections, as well as the 6 water surface elevations at which discharge was computed.

The Energy Equation (Equation 2.9) is based on the Law of Conservation of Energy, and is utilized in the Slope-Area Equation to determine the change in hydraulic head (Δ h) between cross-sections. Flowing water has both kinetic and potential energy, and this energy is quantified by velocity head and water surface height above the streambed, respectively. As water flows from high to low elevation, it loses or gains energy due to friction, expansion or contraction, and changes in velocity. The total amount of energy expended is accounted for in the Energy Equation. Assuming that the energy gradient is parallel to the streambed (i.e. assumption for steady uniform flow), the water surface profile between cross-sections is computed in the Slope-Area Equation using the Energy Equation and the principles of the Law of Conservation of Mass.

Equation 2.8

Cowen Method for Estimating Roughness Coefficients

$$n = (n_0 + n_1 + n_2 + n_3 + n_4)\, m$$

n = roughness

n_0 = bed material

n_1 = surface irregularities

n_2 = variations in channel width

n_3 = channel obstructions

n_4 = vegetation

m = sinuosity

Table 2.1 Computation of Manning's *n* using the Cowen Method

Computation of Manning's *n* from the Cowen Method			
Channel Subsection		Right / Left Overbank Subsections	
bed material	0.054	bed material	n/a
surface irregularities	0.001	surface irregularities	0.020
variations in width	0.000	variations in width	0.000
channel obstructions	0.020	channel obstructions	0.004
vegetation	0.000	vegetation	0.100
Total *n*	0.075	Total *n*	0.124

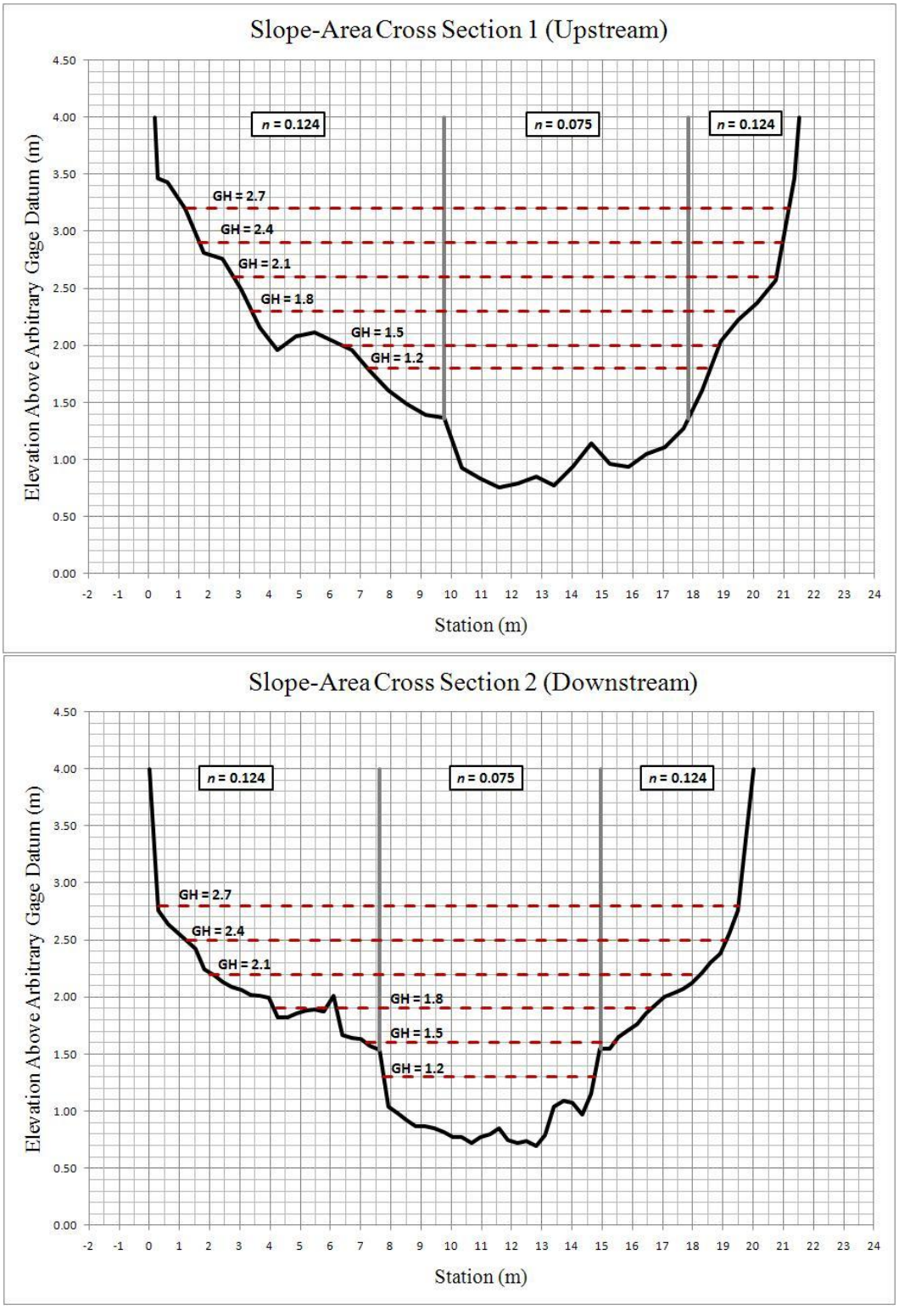

Figure 2.2 Cross-sections for slope-area calculations with water surface elevations and showing Manning's *n* values for different parts of cross-sections.

Equation 2.9

Energy Equation

$$(h + h_v)_1 = (h + h_v)_2 + h_f + h_e$$

h = depth of flow

h_v = velocity head

h_f = energy loss due to friction

h_e = energy loss due to expansion/contraction

The Slope-Area Equation utilizes a value for conveyance (K) that is derived from the Manning's Equation. The K value is a measure of the channel's capacity to pass flow, and is essentially the Manning Equation less the energy gradient variable, or slope (S). Equation 2.10 shows the calculation of K from the Manning Equation.

Equation 2.10

Conveyance Equation

$$K = (1/n)\ A\ R^{2/3}$$

K = Conveyance

n = Manning's roughness coefficient

A = cross sectional area

R = hydraulic radius

The Final Slope-Area Equation to calculate discharge (Equation 2.11) for a reach with two cross-sections is shown below. This final equation also contains a coefficient that describes variations in velocities (α), and represents the ratio between true velocity head and the mean velocity along a cross-section. Equation 2.11 also accounts for expansion and contraction losses using a coefficient (k). Calculations of discharge using the Final Slope-Area Equation are computed by the Slope-Area Computation Program (SAC), a hydraulic analysis program developed by the U.S. Geological Survey. This program was specifically designed to compute discharge and hydraulic characteristics of channels using the methods and equations in Dalrymple and Benson (1967). Hydraulic properties such as area, width, hydraulic radius, velocity, and Froude number are calculated in SAC for each slope-area cross-section.

Equation 2.11

The Final Slope-Area Equation to Calculate Discharge

$$Q = K_2 \sqrt{\frac{\Delta h}{(K_2 / K_1) L + (K_2^{\,2} / 2gA_2^{\,2}) [-\alpha_1 (A_2 / A_1)^2 (1-k) + \alpha_2(1-k)]}}$$

Q = discharge

K = conveyance

L = length of reach

g = gravity

A = cross sectional area

α = velocity head coefficient

Δ h = change in velocity head

k = expansion/contraction coefficient

2.4 Flow Frequency Analysis

The second question in this thesis research is how often do particle mobilizing discharges occur? After threshold discharges are estimated, a flow frequency curve is developed to relate the computed discharge values to a recurrence interval. Because Cheaha Creek is an ungaged stream, peak discharge frequencies are estimated using regression equations developed by the U.S. Geological Survey (USGS) for small rural streams in Alabama (Hedgecock, 2004). The equations are based on peak discharge data at 43 rural gaging stations, each with 10 or more years of discharge record. Separate equations were developed for different regions of the state that exhibit similar physiographic characteristics, and the piedmont regional equation was used for this thesis. Hedgecock's regression equations for small rural streams were exclusively developed for estimating recurrence intervals of 2, 5, 10, 25, 50, 100, 200, and 500 years for ungaged, rural streams with drainage basins of less than 15 mi^2 (38.85 km^2). Cheaha Creek's upper drainage basin meets these requirements, and these regression equations are well suited for modeling flow frequency in Cheaha Creek.

CHAPTER 3

3.0 RESULTS

3.1 Introduction

This thesis research investigates the frequency and magnitude of threshold discharges required to initiate motion of coarse sediment particles in Cheaha Creek, a headwater stream located in the Talladega Mountains of northeastern Alabama and uses the findings to help determine denudation rates for the Talladega Range. The previous chapter detailed the methods employed for estimating discharge, competent particle size, and flood frequency. This chapter provides a comprehensive review of the results of these calculations, thorough descriptions of each of the six study reaches including qualitative characteristics, grain size distributions, channel cross-section geometry, and hydraulic properties used for discharge, shear stress, and Costa competence calculations. Figure 3.1 shows the location of study reaches as well as the longitudinal profile of the channel bed. Water surface profiles are also shown in this figure and are discussed in greater detail later in the chapter.

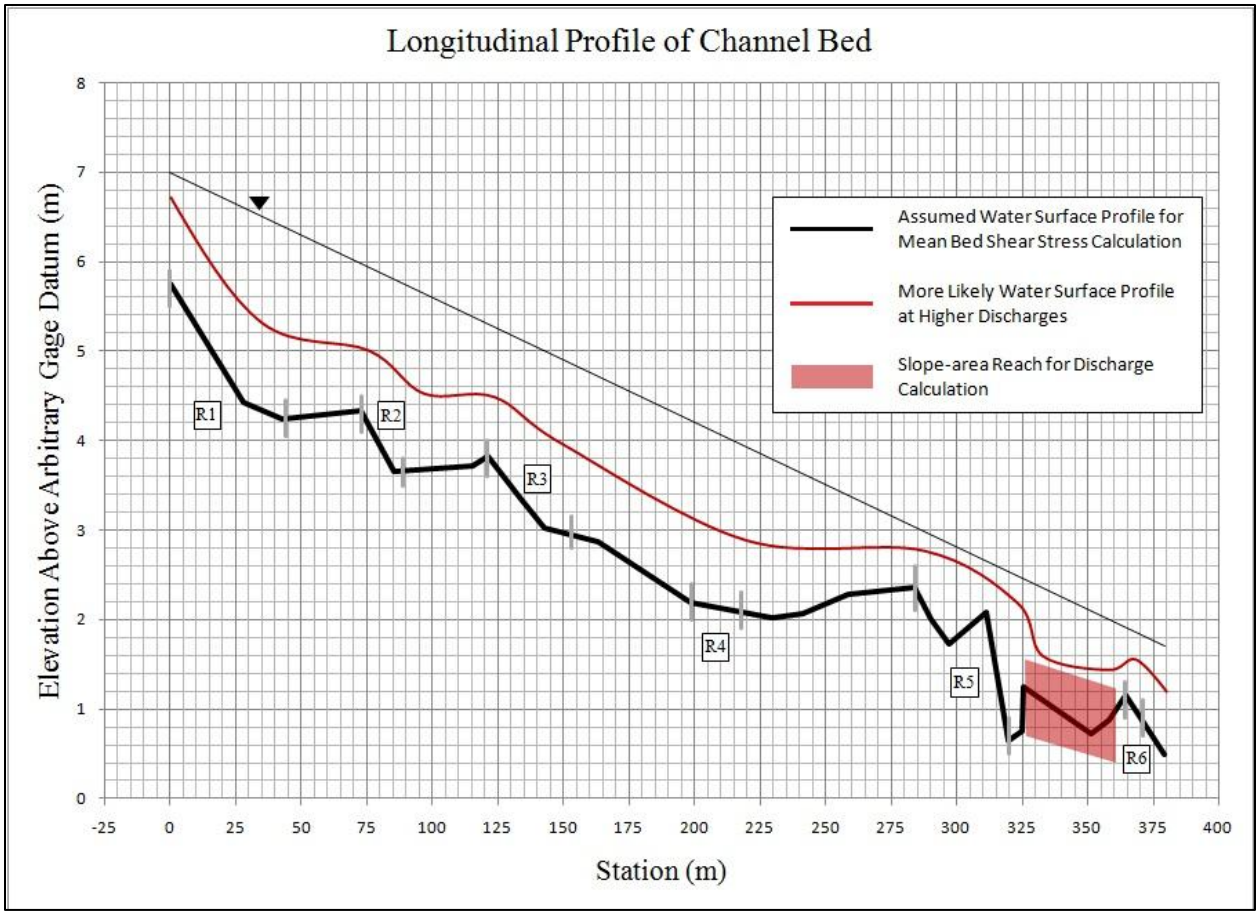

Figure 3.1 Longitudinal profile of the channel bed and Study Reaches.

3.2 Study Reaches

Field data and hydraulic computations are conducted for six Study Reaches within the Study Section, and each reach is detailed below. The beginning of the Study Section is surveyed as river station 0 meters and station numbers increase in the downstream direction, terminating at station 376.

3.2.1 Study Reach 1(river station 0 - 44)

Study Reach 1 (Figure 3.5) is the farthest upstream and marks the beginning of the Study section. The cross-section used in the mean bed shear stress computation (Figure 3.2) was

surveyed at river station 0, and hydraulic properties are shown in Table 3.1. The reach is subdivided by 6 features that produce differences in morphology and hydraulics. The reach begins at river station 0 with a cascade portion as defined by Montgomery and Buffington (1997), where "tumbling jet and wake flow occurs both over and around individual large clasts." Coarse sediment grains are imbricated (Figure 3.6) and irregularly deposited throughout this portion. At station 17 the reach transitions into a moderate velocity pool just below a transverse bedrock outcrop on the downstream right bank. A distinct fine grain deposit is also located below this outcrop, and bulk sediment samples were collected from it. The pool extends to station 29 and is interrupted there by another bedrock outcrop. Coarse sediment grains are deposited along both sides of this feature. Another pool extends below the outcrop to station 44 where it is interrupted by yet another bedrock outcrop, marking the end of Study Reach 1. Coarse sediment grains are found throughout the reach, however the largest accumulation is found in the cascade portion at the beginning of the reach. The reach narrows downstream from a bankfull width of 10.8 m at the origin to 8.5 m at its terminus. The reach bed slope is 0.035, determined from a longitudinal survey of the channel bed. Particle size analysis was conducted for both coarse grain (Figure 3.13) and distinct fine grain deposits (Figure 3.12) in Study Reach 1. This reach exhibited the largest grain size D_{50abc}, D_{84abc}, and D_{90abc} of all the study reaches (Table 3.2). Five bulk samples were taken from distinct deposits located downstream of bedrock outcrops and large alluvial clasts, and one bulk sample was taken from a bar deposit in the middle of the last pool at station 35. The pools in Study Reach 1 mark distinct breaks in gradient and clearly provide energy dissipation at low flows.

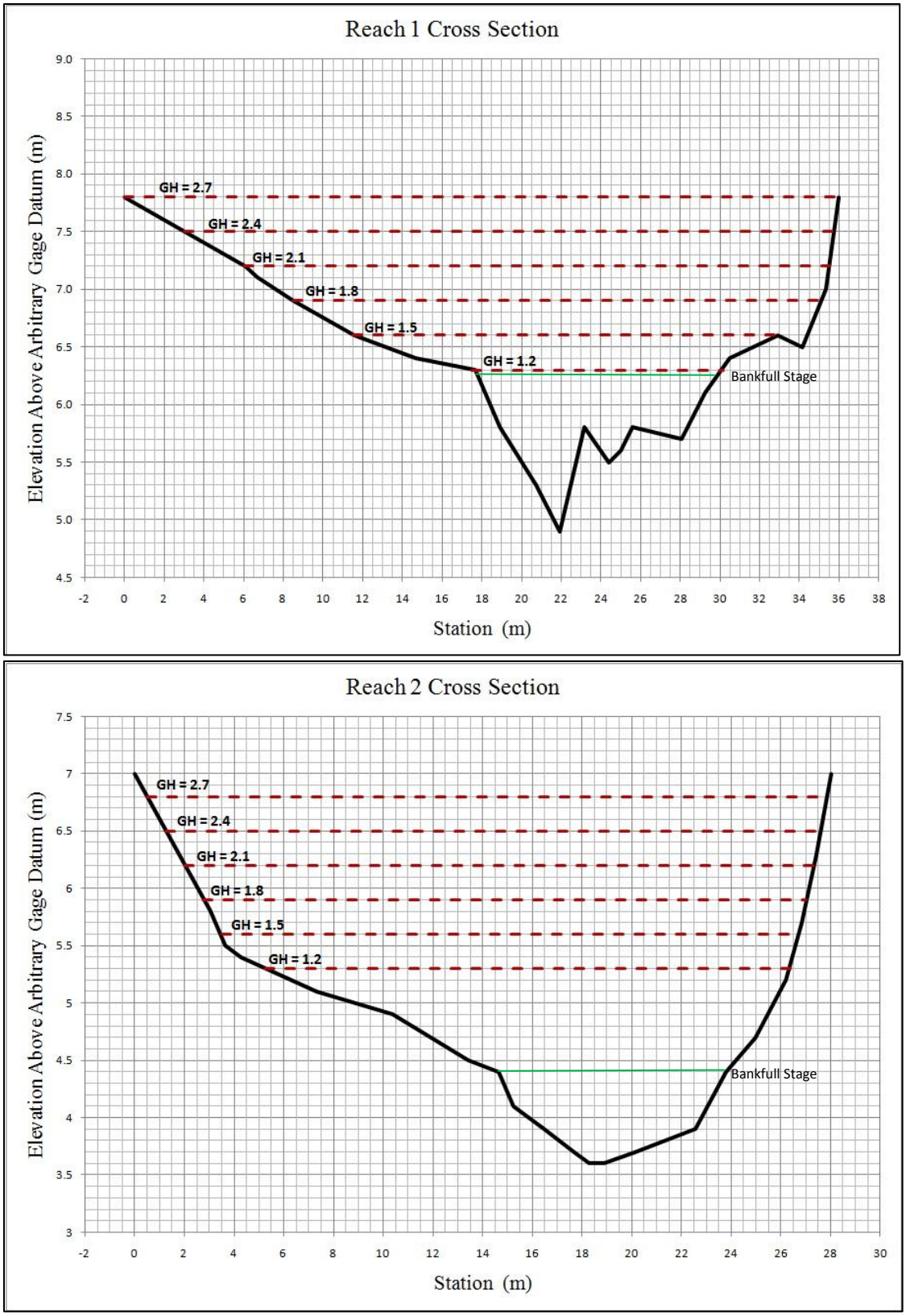

Figure 3.2 Study Reach 1 and 2 cross-sections with water surface elevations

3.2.2 Study Reach 2 (river station 73 - 89)

Study Reach 2 (Figure 3.7) is characterized as step-pool by the Montgomery and Buffington classification scheme (1997), and contains both bedrock and alluvial steps. The cross-section for mean bed shear stress calculations was surveyed at station 73 (Figure 3.2), and hydraulic properties are shown in Table 3.1. Study Reach 2 begins at river station 73 just upstream of a large bedrock outcrop. This large outcrop spans the width of the channel, but has been eroded down on the channel margins so that all water at low flow is directed around the outcrop, forming two chutes on either side. The chute on the left bank is void of sediment, but the right chute contains imbricated cobble to boulder size clasts. The outcrop exhibits a crescent shaped quasi-pothole on the right side, as well as a shallow depression on its crest, both evidence of abrasive erosion and possible plucking (Figure 3.7). Below the outcrop there is a small pool from station 81 - 85 containing alluvial clasts, and at station 85 the coarse grains accumulate to form a channel spanning alluvial step. A distinct fine grain deposit is located at station 86 on the left bank below the step and was bulk sampled for particle size analysis. The reach ends at station 89 with a large colluvial boulder causing coarse grains to accumulate on its upstream side. The reach expands from 8.8 m at station 73 to 10.1 m at station 89, and has a bed slope of 0.055.

3.2.3 Study Reach 3, (river station 121 - 153)

Study Reach 3 (Figure 3.8) includes both step-pool and cascade portions as defined by Montgomery and Buffington (1997). The cross-section for mean bed shear stress calculations was surveyed at station 121 (Figure 3.4), and hydraulic properties are shown in Table 3.1.This

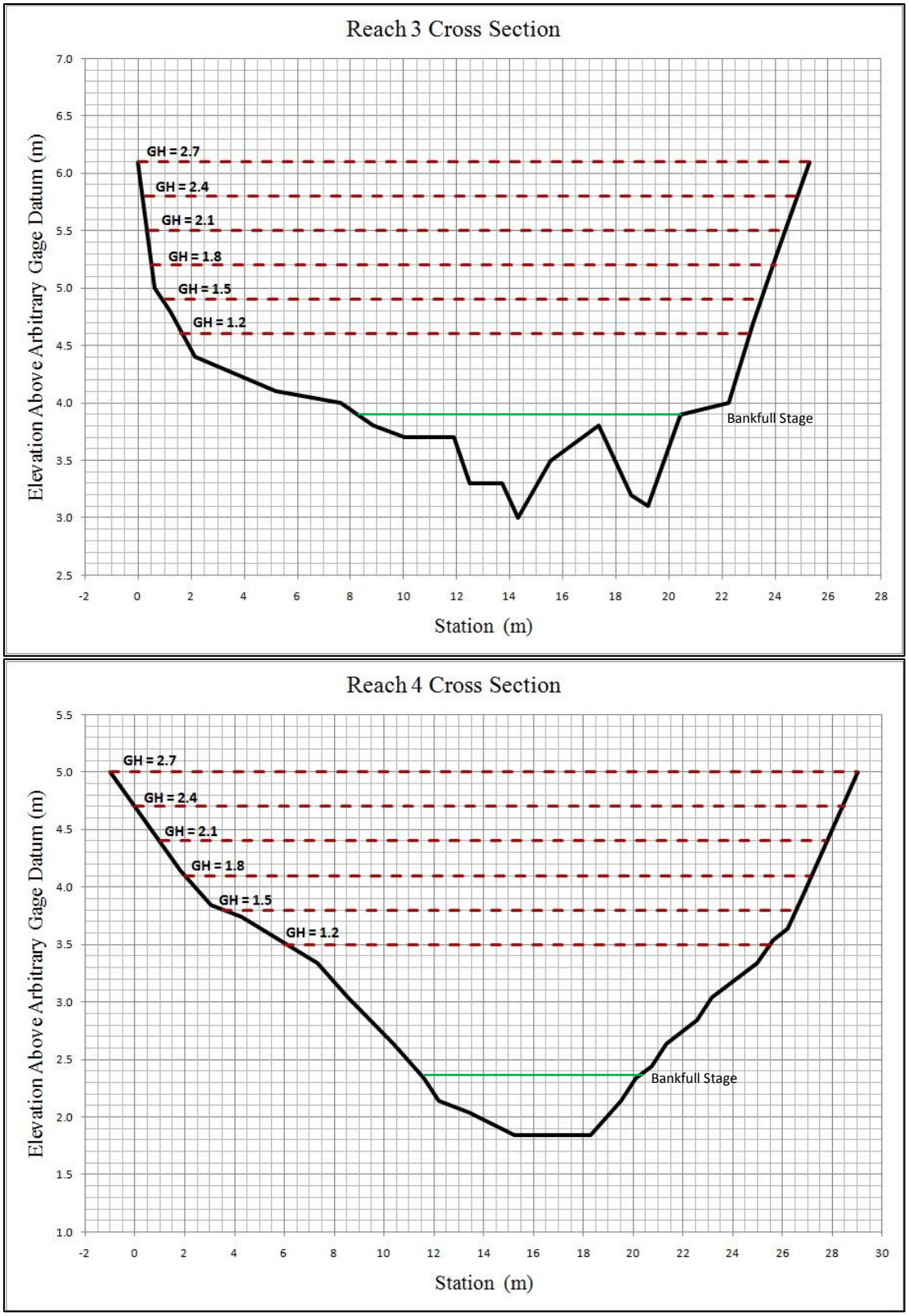

Figure 3.3 Study Reach 3 and 4 cross-sections with water surface elevations.

reach begins at station 121 at the top of a very large colluvial boulder that nearly spans the entire width of the channel. This colluvial boulder forces flow around it, forming two chutes similar to the bedrock outcrop in Study Reach 2. There is a pool below this large boulder from station 122 - 127, and a distinct fine grain longitudinal bar is located in this pool. Bulk sediment samples were taken from this deposit for particle size analysis. At station 129 there is a mixed bedrock-alluvial step containing coarse boulder clasts. The bedrock outcrop in this step has been eroded in three locations, and water is directed through these areas at low flow. From station 129 - 149 the reach exhibits cascade characteristics, with imbricated coarse grains and shallow bedrock protrusions irregularly located throughout. Two distinct fine grain deposits located on the left bank were sampled in this cascade portion. At station 149 an alluvial step composed of cobbles to small boulders transverses the channel, with a distinct fine grain deposit on its lee side from which sediment samples were taken. The bankfull width in Study Reach 3 expands from 9.9 m at station 121 to 11.0 m at station 153, and the reach exhibits a bed slope of 0.017.

3.2.4 Study Reach 4 (river station 199 - 218)

Study Reach 4 (Figure 3.9) is composed solely of alluvial step morphologies. The cross-section for mean bed shear stress calculations was surveyed at station 199 (Figure 3.3), and hydraulic properties are shown in Table 3.1. This reach begins at station 199, 3 m upstream of the first alluvial step. This step spans the entire channel width, but the grain sizes vary along the cross-section. The channel margin grains consist of small to medium boulders, but the clasts in the center of the channel are limited to small to large cobbles. The center of the channel conveys the majority of water at low flow. A moderate velocity pool containing a few irregularly spaced cobbles is below this step and extends from station 202 - 214. Two distinct fine grain deposits

are located in this pool and samples were taken from both. An alluvial step composed of imbricated cobble - boulder particles marks the end of the pool at station 214. This step is not perpendicular to the channel as are most alluvial steps in the study reaches, but is skewed downstream on the left bank. The step joins a bedrock outcrop on the right bank, which may be a factor in the skewness of the step. At higher flows it is possible that the outcrop on the right bank backs up water, causing effective flow to be directed toward the left bank. This would produce higher competency values on the left bank, resulting in the observed skewness. A distinct fine grain deposit is found on the downstream side of the bedrock outcrop, and a bulk sediment sample was collected from it. The bankfull width in Study Reach 4 remains uniform at 7.9 m, and the bed slope is the lowest of all reaches at 0.003.

3.2.5 Study Reach 5 (river station 284 - 320)

Study Reach 5 (Figure 3.10) includes both step-pool and cascade sequences as defined by Montgomery and Buffington (1997). The cross-section for mean bed shear stress calculations was surveyed at station 284 (Figure 3.4), and hydraulic properties are shown in Table 3.1. Very large colluvial boulders and bedrock outcrops are common in this reach. This reach begins at the top of a bedrock outcrop leading into a cascade sequence. At low flow, water falls over a 0.5 m bedrock lip and is then directed around both sides of a large colluvial boulder located at station 289. Many imbricated cobble - boulder size grains along with several bedrock outcrops are irregularly distributed throughout the cascade sequence. The bedrock outcrops are worn smooth on their crests showing signs of abrasive erosion. The cascade sequence extends to station 308, where a pool forms due to a transverse bedrock outcrop located at station 316. The outcrop is quite thick and forms small pools between rock protrusions above the water surface at low flow.

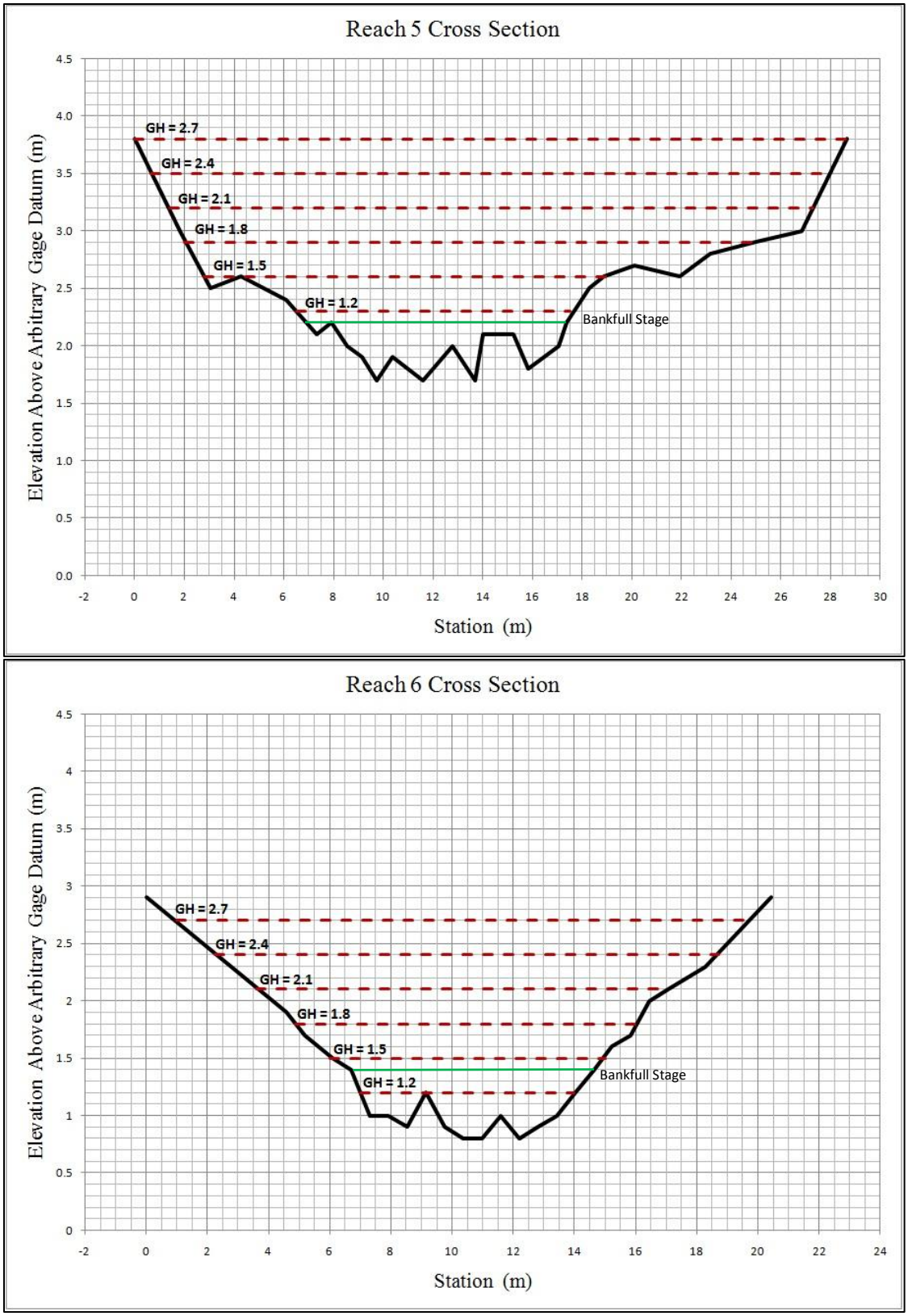

Figure 3.4 Study Reach 5 and 6 cross-sections with water surface elevations.

Study Reach 5 ends at station 320 at the terminus of the bedrock outcrop. Several distinct deposits are found in this reach and a total of 7 bulk sediment samples were taken, usually behind colluvial boulders and bedrock outcrops. The bankfull width in Study Reach 5 contracts from 10.9 m at station 284 to 9.4 at station 320, and the reach exhibits a bed slope of 0.039.

3.2.6 Study Reach 6 (river station 364 - 371)

Study Reach 6 is the shortest reach in this research, and is characterized as a single bedrock step-pool sequence Figure 3.11. The cross-section for mean bed shear stress calculations was surveyed at station 364 (Figure 3.4), and hydraulic properties are shown in Table 3.1. This reach begins at the crest of a bedrock outcrop. The outcrop is eroded on the right bank and an accumulation of cobble to small boulder size grains are located just downstream of this eroded notch. On the left side of the channel the erosion of bedrock is more evenly distributed leaving a smoother and wider flow path, but just below the bedrock there is a relatively deep plunge pool and hydraulic jump. Most of the water flows on this side of the channel at low flow. A distinct fine grain deposit is located at the end of the reach at station 371, just downstream of a small outcrop. The bankfull width in Study Reach 6 remains uniform at 8.2 m, and the bed slope is 0.044.

Figure 3.5 Study Reach 1 at low flow looking upstream.

Figure 3.6 Clast imbrication in the downstream direction (to right).

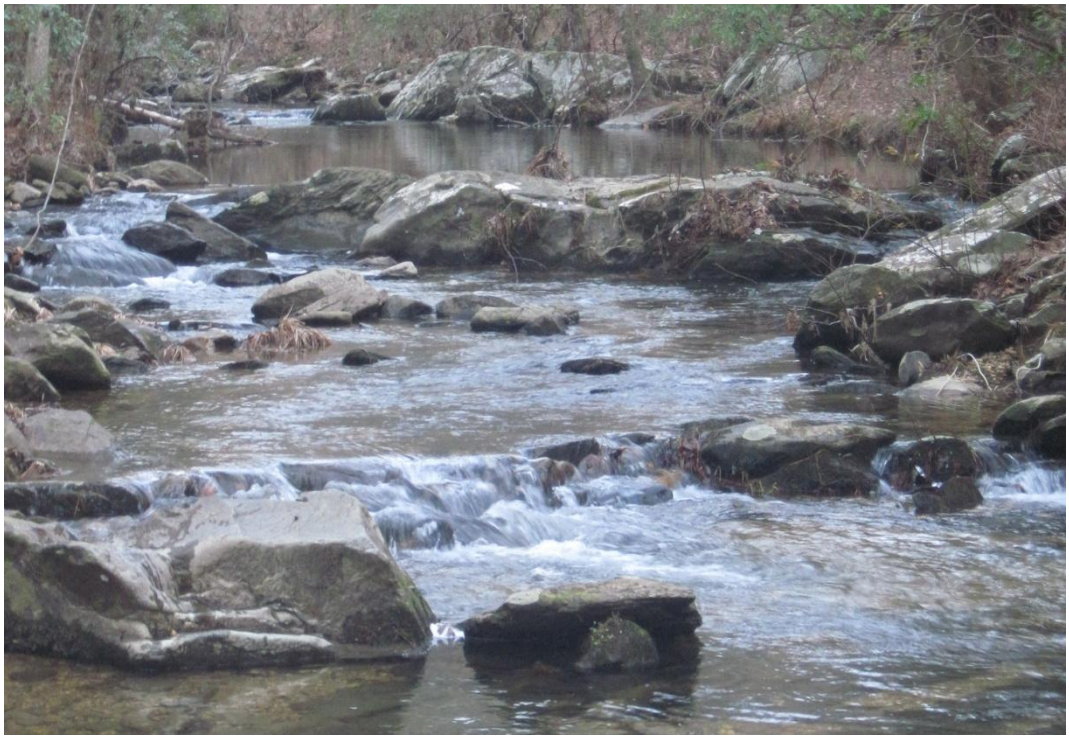

Figure 3.7 Study Reach 2 at low flow looking upstream.

Figure 3.8 Study Reach 3 at low flow looking upstream.

Figure 3.9 Study Reach 4 at low flow looking upstream.

Figure 3.10 Study Reach 5 at low flow looking upstream.

Figure 3.11 Study Reach 6 at low flow looking upstream with Study Reach 5 in the background.

Table 3.1 Hydraulic properties for all study reaches calculated by WSPRO.

Hydraulic Properties for Cheaha Creek Study Reaches					
Reach 1					
Gage Height (m)	Area (m^2)	Wetted Perimeter (m)	Hydraulic Radius (m)	Top Width (m)	Mean Depth (m)
1.2	7.62	12.80	0.60	12.19	0.62
1.5	12.73	23.47	0.54	22.86	0.56
1.8	20.25	27.43	0.74	26.52	0.76
2.1	28.80	30.48	0.94	29.57	0.97
2.4	38.37	34.44	1.11	33.22	1.15
2.7	49.05	37.49	1.31	35.97	1.36
Reach 2					
Gage Height (m)	Area (m^2)	Wetted Perimeter (m)	Hydraulic Radius (m)	Top Width (m)	Mean Depth (m)
1.2	17.93	21.34	0.84	20.73	0.87
1.5	24.71	23.77	1.04	23.16	1.07
1.8	31.96	24.99	1.28	24.08	1.33
2.1	39.48	26.21	1.51	25.30	1.56
2.4	47.38	27.43	1.73	26.21	1.81
2.7	55.55	28.65	1.94	27.43	2.03
Reach 3					
Gage Height (m)	Area (m^2)	Wetted Perimeter (m)	Hydraulic Radius (m)	Top Width (m)	Mean Depth (m)
1.2	17.65	22.25	0.79	21.34	0.83
1.5	24.34	23.77	1.02	22.56	1.08
1.8	31.40	24.99	1.26	23.47	1.34
2.1	38.65	25.91	1.49	24.38	1.58
2.4	46.17	26.82	1.72	24.99	1.85
2.7	53.88	27.74	1.94	25.30	2.13
Reach 4					
Gage Height (m)	Area (m^2)	Wetted Perimeter (m)	Hydraulic Radius (m)	Top Width (m)	Mean Depth (m)
1.2	19.69	20.12	0.98	19.81	0.99
1.5	26.29	24.08	1.09	23.47	1.12
1.8	33.72	25.91	1.30	25.30	1.33
2.1	41.81	28.04	1.49	27.13	1.54
2.4	50.17	28.96	1.73	27.74	1.81
2.7	58.62	29.57	1.98	27.74	2.11
Reach 5					
Gage Height (m)	Area (m^2)	Wetted Perimeter (m)	Hydraulic Radius (m)	Top Width (m)	Mean Depth (m)
1.2	4.37	12.19	0.36	11.58	0.38
1.5	8.55	18.90	0.45	17.98	0.48
1.8	15.05	24.99	0.60	24.38	0.62
2.1	22.85	27.43	0.83	26.52	0.86
2.4	31.12	28.96	1.07	28.04	1.11
2.7	39.85	30.18	1.32	28.65	1.39
Reach 6					
Gage Height (m)	Area (m^2)	Wetted Perimeter (m)	Hydraulic Radius (m)	Top Width (m)	Mean Depth (m)
1.2	1.86	7.32	0.25	7.01	0.27
1.5	4.27	9.45	0.45	9.14	0.47
1.8	7.43	11.89	0.63	11.28	0.66
2.1	11.15	14.33	0.78	13.72	0.81
2.4	15.89	17.37	0.91	16.76	0.95
2.7	21.37	19.81	1.08	19.20	1.11

3.2.7 Particle Size Analysis

A particle size analysis is conducted for this research to characterize both the size of sediment grains and the distribution of size classes within the study reaches of Cheaha Creek. In order to answer the overarching research questions regarding frequency and magnitude of particle mobilizing discharges, it is necessary to first determine the sizes of clasts in each reach.

The particle size distributions are completed for two primary sediment populations - coarse grains, which dominate the channel bed, and fine-grain-distinct deposits usually limited to areas on the lee side of large boulders and bedrock outcrops. All three principal axes (a,b,c) are measured and shear stress determined for different grain size classes (Table 3.2). This research presents a range of critical shear stress values for initial motion of sediment clasts for each study reach derived from the particle size analysis of all three principal axes.

Figure 3.13 graphically shows the coarse grain size distributions for all study reaches. The D_{50a} for all reaches ranges from 461 - 924 mm, with an average of 652 mm. This places all *a-axis* D_{50} particles in the small to medium boulder class. The D_{84a} for all reaches ranges from 824 - 1389 mm, with a reach average of 1013 mm. The D_{90a} ranges from 927 - 1490 mm and averaged 1159 mm. A downstream fining of the *a-axis* is observed where Reach 1 consistently exhibits the largest class sizes, and Reach 6 shows the smallest of all the study reaches. The D_{50b} for all reaches ranges from 252 - 353 mm, with an average of 293 mm. This places the *b-axis* D_{50} particles in the large cobble to small boulder class size. The D_{84b} and D_{90b} ranges from 423 - 545 mm and 462 - 599 mm, respectively. Reach 1 again exhibits the largest grain diameters. The D_{50c} ranges from 74 - 106 mm and averages 83 mm. This places the *c-axis* D_{50} particles in the small to medium cobble class size. D_{84c} and D_{90c} ranges from 136 - 242 mm and 189 - 329 mm, respectively. Reach 1 shows the largest grain diameters, and Reach 6 shows some of the lowest

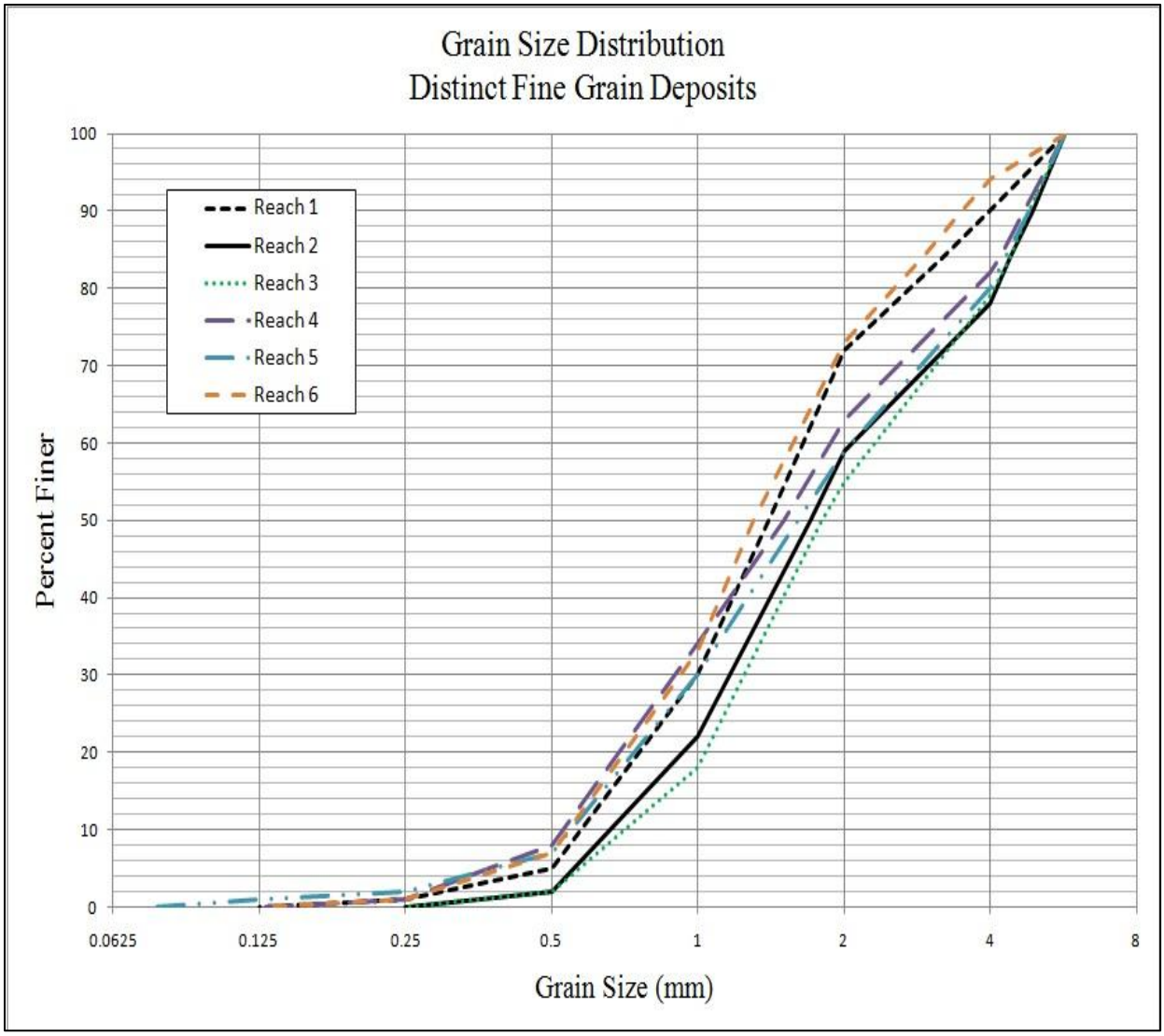

Figure 3.12 Grain size distribution for distinct fine grain deposits in all reaches.

values. The fine grain distinct deposits are bulk sampled, and a particle size analysis is conducted for the *b-axis* diameter of these grains (Figure 3.12). Results from these samples indicate that the cumulative D_{50}, D_{84}, and D_{90} are 1.5, 4.0, and 4.6 mm, respectively. This is a substantial decrease in diameter from the coarse grain size distributions.

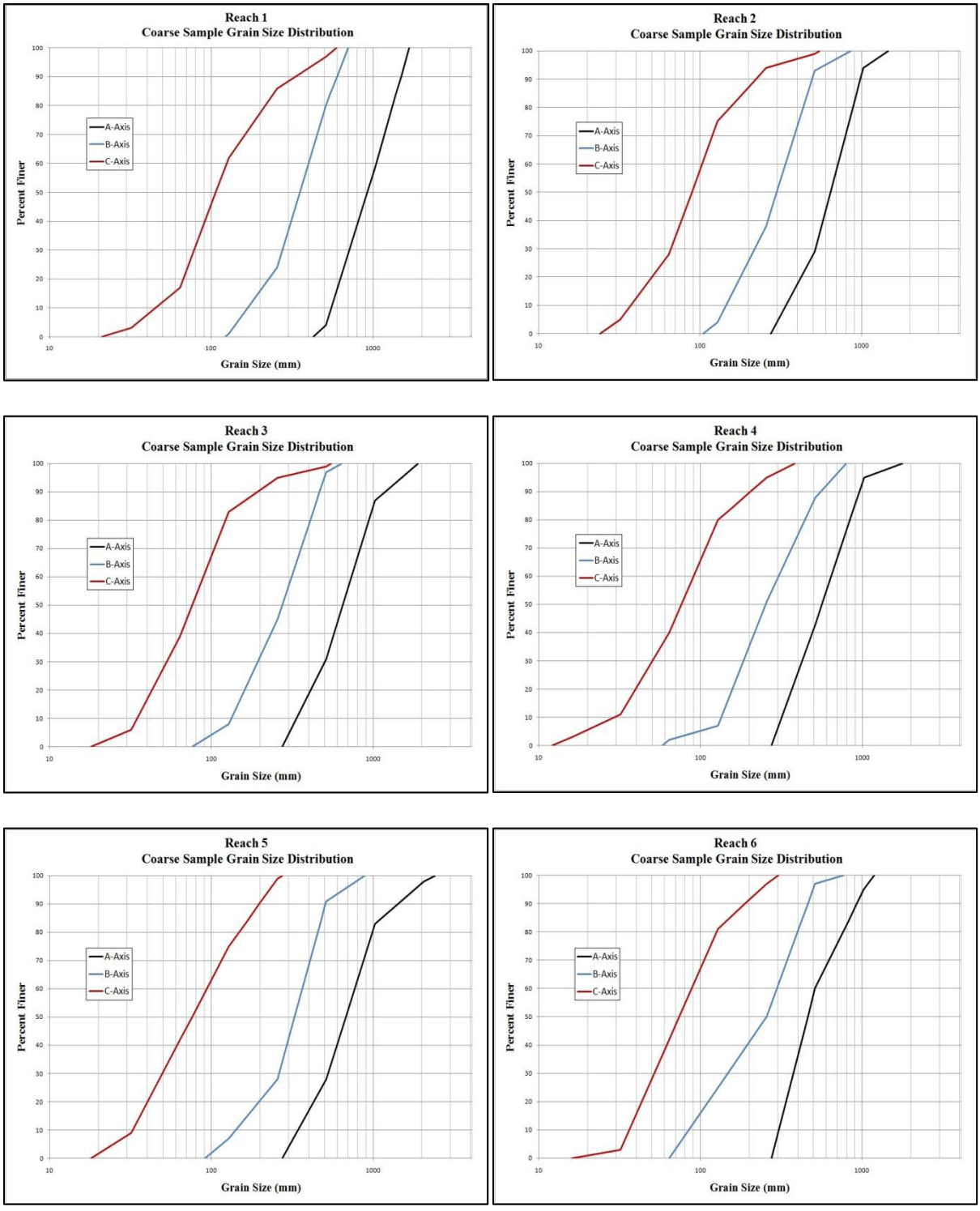

Figure 3.13 Particle size distributions of A, B, and C axes of coarse grains.

Table 3.2 Coarse grain size classes

Coarse Grain Size Classes									
Reach	A-Axis			B-Axis			C-Axis		
	D50	D84	D90	D50	D84	D90	D50	D84	D90
1	924	1389	1490	353	545	599	106	242	329
2	641	920	981	298	457	493	89	178	221
3	648	987	1180	273	431	466	76	136	192
4	562	884	958	252	475	551	76	154	203
5	676	1072	1415	326	474	506	76	166	197
6	461	824	927	256	423	462	74	146	189
Reach Mean	652	1013	1159	293	468	513	83	170	222

3.3 Slope-Area Calculations

Discharges in Cheaha Creek are estimated using the Slope-Area Equation. The Slope-Area Equation for calculating discharge utilizes an equation based on steady uniform flow requiring channel geometry characteristics, Manning's roughness values (Manning's *n*), and energy gradient (Dalrymple and Benson, 1967). The two cross-sections used for the slope area method along with the water surface elevations at which discharge was calculated are shown in Figure 2.2. This research utilized the USGS SAC program to compute discharge for the Slope-Area Equation. The SAC program requires channel geometry data, roughness values, and water surface elevations to compute discharge. Because SAC is a one dimensional flow model, all topographic data used in SAC must be tied to the same vertical datum, but different cross-sections are not required to be in the same horizontal coordinates, only the distance between them is needed. For this research an arbitrary vertical datum is developed from the survey of the channel bed. This datum, hereafter referred to as gage datum, has a value of 0.0 m at an arbitrary

Table 3.3 Cross-section hydraulic properties used in slope-area calculations.

Hydraulic Properties of Slope-area Cross-sections for Discharge Calculations						
Slope-Area Cross-section 1 (Upstream)						
Gage Height (m)	Discharge (m^3/s)	Area (m^2)	Wetted Perimeter (m)	Hydraulic Radius (m)	Velocity (m/s)	Froude
1.2	4.2	6.97	11.28	0.62	0.6	0.24
1.5	8.5	10.68	15.24	0.70	0.8	0.29
1.8	14.2	15.51	17.37	0.89	0.9	0.30
2.1	21.7	20.90	18.90	1.11	1.0	0.31
2.4	31.4	26.66	20.73	1.29	1.2	0.32
2.7	43.1	32.70	21.64	1.51	1.3	0.33
Slope-Area Cross-section 2 (Downstream)						
Gage Height (m)	Discharge (m^3/s)	Area (m^2)	Wetted Perimeter (m)	Hydraulic Radius (m)	Velocity (m/s)	Froude
1.2	4.2	2.92	7.32	0.40	1.4	0.71
1.5	8.5	5.11	8.84	0.58	1.6	0.67
1.8	14.2	8.18	13.41	0.61	1.7	0.68
2.1	21.7	12.63	17.37	0.73	1.7	0.63
2.4	31.4	17.93	19.20	0.93	1.8	0.56
2.7	43.1	23.60	20.42	1.16	1.8	0.53

point 0.8 m below the thalweg of Study Reach 6. SAC is typically used in applications where the profile of the water surface is known, from either visual observation during a flood or accurate high water marks. However, due to lack of these data for this research the water surface gradient is assumed to be equal to the gradient of the channel bed between slope-area cross-sections. The SAC program requires the gradient value to be input as the fall between cross-sections (Δh), and for this research the slope-area cross-sections show $\Delta h = 0.45$ m. The SAC program allows for the channel to be divided into subsections for breaks in surface roughness. Manning's roughness coefficients (n) are calculated using the Cowen iterative technique (Cowen, 1956) and three sub-sections per cross-section are given roughness values. Table 2.1 shows the calculation of roughness for each sub-section. For both cross-sections the channel is given a roughness of n = 0.075, and both overbanks were determined to be n = 0.124.

The SAC program calculates discharges for 6 water surface elevations above the gage datum in increments of 0.3 m (Figure 3.14). The Δh between cross-sections is assumed to remain

constant for all calculations, but the actual Δh during a flood would most likely vary between cross-sections at different discharges. Hydraulic properties are calculated by SAC and output along with the discharge values. Table 3.3 shows the hydraulic properties at each discharge calculated by SAC. Even though the discharge values calculated using the Slope-Area Equation are computed for a reach comprising only 10% of the overall Study Section, these discharges are assumed to translate throughout all of the study reaches. This assumption is considered valid because there are no tributaries contributing flow in the Study Section that would increase

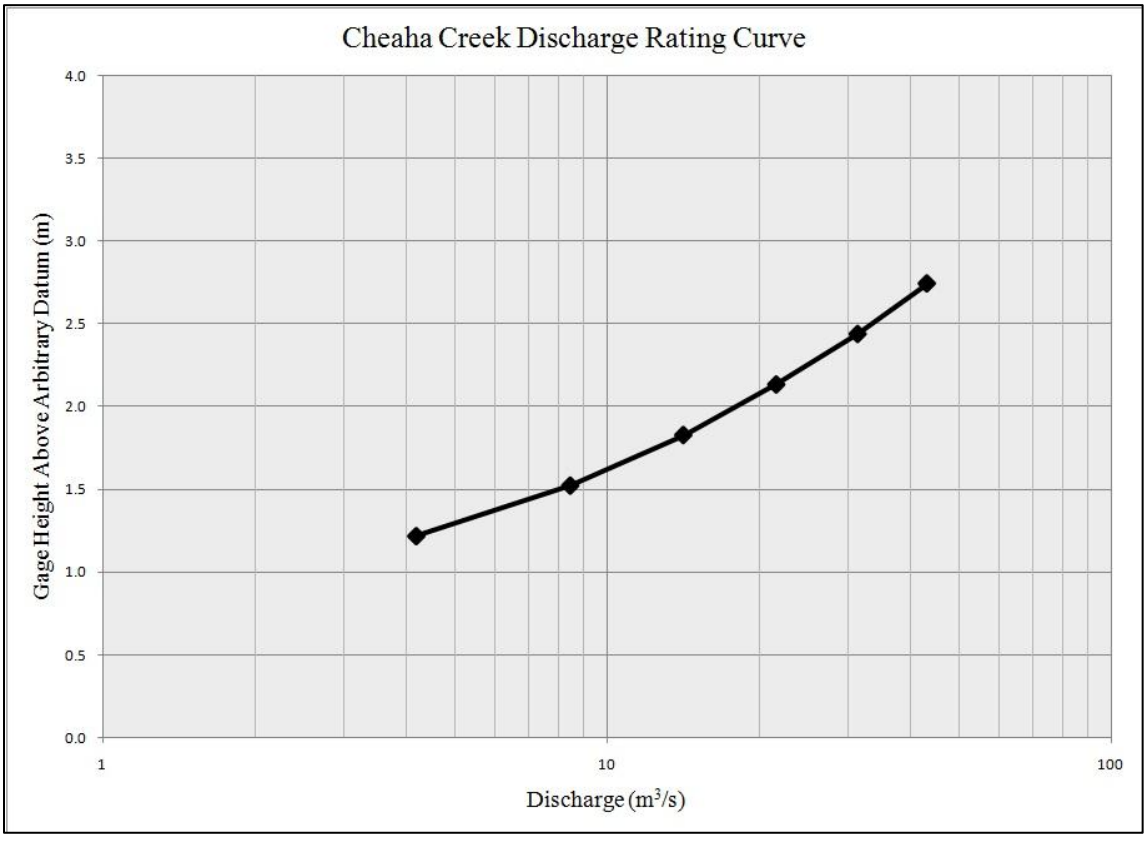

Figure 3.14 Discharge rating curve developed from the slope-area calculation.

discharge at a point not shared by all study reaches. However, it is likely that surface runoff would cause a cumulative increase in discharge to points farther downstream compared to other points upstream with less drainage area. If this does occur, it is assumed to be less discharge than

the overall error encountered by modeling streamflow without a known water surface profile. Therefore it is assumed that at a gage height (GH) of 1.2 m, discharge at each of the study reaches is 4.2 m^3/s (148 cfs), GH of 1.5 = 8.5 m^3/s (299 cfs), GH of 1.8 = 14.2 m^3/s (501 cfs), GH of 2.1 = 21.7 m^3/s (766 cfs), GH of 2.4 = 31.4 m^3/s (1111 cfs), and GH of 2.7 = 43.1 m^3/s (1524 cfs).

Figures 3.2 - 3.4 show the study reach cross-sections and the water surface elevations at each gage height translated through the Study Section. These water surface elevations were calculated by assuming that the slope of the water surface is equal to the average bed slope of the channel bed (0.014) (Figure 3.1). This assumption was made due to the lack of flood data. Visual observations of a flood or accurate high water marks are the best indicators of a water surface profile. There are hydraulic modeling programs available that will compute an estimated water surface profile, but their use is beyond the scope of this research. Issues regarding using an average slope as the water surface profile are discussed in Chapter 4.

3.4 Estimates of Threshold Discharges and Competent Particle Sizes

Results from these calculations are found in Table 3.4. The range of largest *b-axis* of competent grains are as follows: Study Reach 1 - 174 to 445 mm, Study Reach 2 - 258 to 715 mm, Study Reach 3 - 244 to 760 mm, Study Reach 4 - 305 to 753 mm, Study Reach 5 - 95 to 456 mm, and Study Reach 6 - 95 to 459 mm. When results of the Costa Method are compared to the adjusted Shields Method later in this chapter, only grain sizes for Study Reaches 1, 5, and 6 are compared. Average velocity is also computed with the Costa method using particle size as the independent variable. For this research, the calculated competent particle size is entered into the equation to derive average velocity (Equation 2.1), and the results are found in Table 3.4.

Discharge is then computed using the Continuity Equation (Equation 2.3). As expected, computed discharges were much greater in reaches 2, 3, and 4 from overestimating cross-sectional area. In reaches 1, 5, and 6 discharges ranged from 2.5 m^3/s (88 cfs) at GH = 1.2 to 172 m^3/s (6074 cfs) at GH = 2.7.

3.5 Estimates of Particle Entrainment

In addition to utilizing the Costa approach to determine threshold discharges required to initiate motion of coarse sediment grains, this research also employs tractive force equations that have been widely used in sediment transport studies (Shields, 1936; Miller *et al*., 1977; Wiberg and Smith, 1987; Komar, 1987; Buffington and Montgomery, 1997). Mean bed shear stress (τ_o) is calculated for all study reaches as well as the slope-area cross-sections using Equation 2.4. Figure 3.15 shows the results of τ_o computations. Reaches 2, 3, and 4 exhibit much greater values for τ_o, and this is a result of overestimating cross-sectional area for a given discharge. A larger area of flow increases the hydraulic radius term in Equation 2.4, resulting in greater τ_o values. Reaches 1, 5, 6, and both slope-area cross-sections demonstrate more reliable values. It is worth noting that τ_o values are variable between reaches at lower discharges, likely due to irregularities and differences in channel bed topography. However as discharges increases there is less local variability between cross-sections, and increases in τ_o become more uniform (Figure 3.15). Calculated mean bed shear stress values for all study reaches and slope-area cross-sections are as follows: Study Reach 1 - 82 to 180 N/m^2, Study Reach 2 - 115 to 266 N/m^2, Study Reach 3 - 109 to 267 N/m^2, Study Reach 4 - 134 to 272 N/m^2, Study Reach 5 - 49 to 181 N/m^2, Study Reach 6 - 35 to 148 N/m^2, Upstream slope-area cross-section - 85 to 208 N/m^2, Downstream slope-area cross-section - 55 to 159 N/m^2.

Table 3.4 Discharge and competency results using the Costa Method.

Costa Method - Discharge and Compentency Results					
Reach 1					
Gage Height (m)	Competent Particle Size (mm)	Mean Depth (m)	Area (m^2)	Velocity (m/s)	Discharge (m^3/s)
1.2	174	0.62	7.62	2.22	16.9
1.5	152	0.56	12.73	2.08	26.4
1.8	222	0.76	20.25	2.50	50.6
2.1	297	0.97	28.80	2.88	83.0
2.4	365	1.15	38.37	3.18	122.1
2.7	445	1.36	49.05	3.51	172.1
Reach 2					
Gage Height (m)	Competent Particle Size (mm)	Mean Depth (m)	Area (m^2)	Velocity (m/s)	Discharge (m^3/s)
1.2	258	0.87	17.93	2.69	48.2
1.5	331	1.07	24.71	3.04	75.1
1.8	431	1.33	31.96	3.45	110.3
2.1	523	1.56	39.48	3.80	149.9
2.4	624	1.81	47.38	4.14	195.9
2.7	715	2.03	55.55	4.42	245.5
Reach 3					
Gage Height (m)	Competent Particle Size (mm)	Mean Depth (m)	Area (m^2)	Velocity (m/s)	Discharge (m^3/s)
1.2	244	0.83	17.65	2.62	46.2
1.5	336	1.08	24.34	3.06	74.5
1.8	435	1.34	31.40	3.47	108.9
2.1	533	1.58	38.65	3.83	148.0
2.4	641	1.85	46.17	4.19	193.4
2.7	760	2.13	53.88	4.55	245.3
Reach 4					
Gage Height (m)	Competent Particle Size (mm)	Mean Depth (m)	Area (m^2)	Velocity (m/s)	Discharge (m^3/s)
1.2	305	0.99	19.69	2.92	57.4
1.5	351	1.12	26.29	3.13	82.2
1.8	433	1.33	33.72	3.46	116.7
2.1	515	1.54	41.81	3.77	157.5
2.4	625	1.81	50.17	4.14	207.6
2.7	753	2.11	58.62	4.53	265.6
Reach 5					
Gage Height (m)	Competent Particle Size (mm)	Mean Depth (m)	Area (m^2)	Velocity (m/s)	Discharge (m^3/s)
1.2	95	0.38	4.37	1.65	7.2
1.5	126	0.48	8.55	1.89	16.2
1.8	172	0.62	15.05	2.21	33.2
2.1	257	0.86	22.85	2.68	61.3
2.4	348	1.11	31.12	3.11	96.8
2.7	456	1.39	39.85	3.55	141.4
Reach 6					
Gage Height (m)	Competent Particle Size (mm)	Mean Depth (m)	Area (m^2)	Velocity (m/s)	Discharge (m^3/s)
1.2	62	0.27	1.86	1.35	2.5
1.5	123	0.47	4.27	1.88	8.0
1.8	186	0.66	7.43	2.29	17.0
2.1	239	0.81	11.15	2.59	28.9
2.4	288	0.95	15.89	2.84	45.0
2.7	349	1.11	21.37	3.11	66.6

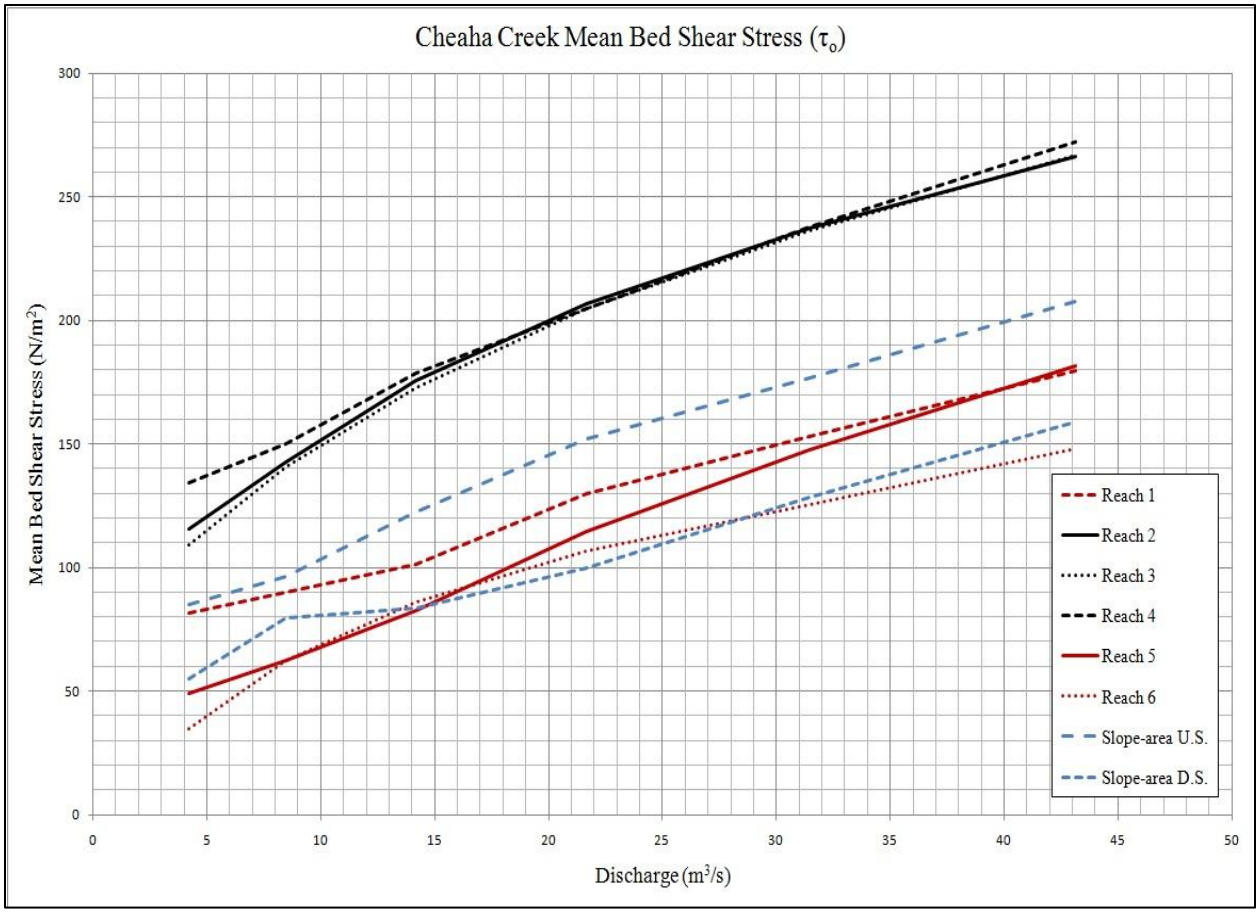

Figure 3.15 Mean bed shear stress at calculated discharges.

Critical shear stress (τ_c) is computed using Equation 2.6 for the D_{50}, D_{84}, and D_{90} grain sizes (*b-axis*) of the fine grain distinct deposits in each reach, and results are shown in Table 3.5. The D_{50}, D_{84}, and D_{90} of the distinct deposits are found to be mobile at all calculated discharges in all study reaches. Ratios of τ_o / τ_c were much greater than 1.0 for all study reaches, and values ranged from 25 - 176. Ratios of τ_o / τ_c were also calculated for each coarse grain axis sample. These data are shown for each axis in Tables 3.6 - 3.8. Ratios reached 1.0 for the *a-axis and b-axis* coarse grain samples only in Study Reaches 2, 3, and 4. The *c-axis* coarse grain sample exhibited ratios greater than 1.0 in all Study Reaches and at most discharges.

Table 3.5 Shear Stress Calculations for Distinct Fine Grain Deposits

Shear Stress Calculations for Distinct Fine Grain Deposits (B-Axis in mm)															
Reach 1															
Discharge (m^3/s)	D50	τ*c	τc	τo	τo / τc	D84	τ*c	τc	τo	τo / τc	D90	τ*c	τc	τo	τo / τc
4.2	1.4	0.045	1.02	81.73	80.14	3.2	0.045	1.42	81.73	57.58	4.0	0.045	1.55	81.73	52.66
8.5				74.48	73.04				74.48	52.47				74.48	47.99
14.2				101.39	99.43				101.39	71.43				101.39	65.33
21.7				129.77	127.25				129.77	91.42				129.77	83.62
31.4				152.99	150.03				152.99	107.79				152.99	98.58
43.1				179.69	176.21				179.69	126.60				179.69	115.79
Reach 2															
Discharge (m^3/s)	D50	τ*c	τc	τo	τo / τc	D84	τ*c	τc	τo	τo / τc	D90	τ*c	τc	τo	τo / τc
4.2	1.7	0.045	1.24	115.41	93.21	4.4	0.045	1.81	115.41	63.71	4.9	0.045	1.89	115.41	61.03
8.5				142.75	115.28				142.75	78.81				142.75	75.49
14.2				175.61	141.82				175.61	96.95				175.61	92.86
21.7				206.87	167.06				206.87	114.20				206.87	109.39
31.4				237.21	191.56				237.21	130.95				237.21	125.43
43.1				266.30	215.06				266.30	147.01				266.30	140.82
Reach 3															
Discharge (m^3/s)	D50	τ*c	τc	τo	τo / τc	D84	τ*c	τc	τo	τo / τc	D90	τ*c	τc	τo	τo / τc
4.2	1.8	0.045	1.31	108.95	83.10	4.4	0.045	1.87	108.95	58.12	4.8	0.045	1.94	108.95	56.13
8.5				140.61	107.24				140.61	75.01				140.61	72.44
14.2				172.54	131.60				172.54	92.04				172.54	88.89
21.7				204.87	156.26				204.87	109.29				204.87	105.55
31.4				236.41	180.32				236.41	126.11				236.41	121.80
43.1				266.80	203.49				266.80	142.32				266.80	137.45
Reach 4															
Discharge (m^3/s)	D50	τ*c	τc	τo	τo / τc	D84	τ*c	τc	τo	τo / τc	D90	τ*c	τc	τo	τo / τc
4.2	1.5	0.045	1.09	134.46	123.06	4.2	0.045	1.65	134.46	81.52	4.7	0.045	1.61	134.46	83.28
8.5				149.95	137.25				149.95	90.92				149.95	92.88
14.2				178.77	163.62				178.77	108.38				178.77	110.73
21.7				204.75	187.40				204.75	124.14				204.75	126.82
31.4				237.94	217.78				237.94	144.26				237.94	147.38
43.1				272.30	249.23				272.30	165.10				272.30	168.66
Reach 5															
Discharge (m^3/s)	D50	τ*c	τc	τo	τo / τc	D84	τ*c	τc	τo	τo / τc	D90	τ*c	τc	τo	τo / τc
4.2	1.6	0.045	1.17	49.19	42.20	4.3	0.045	1.73	49.19	28.42	4.8	0.045	1.81	49.19	27.20
8.5				62.11	53.30				62.11	35.89				62.11	34.34
14.2				82.70	70.96				82.70	47.78				82.70	45.73
21.7				114.42	98.18				114.42	66.11				114.42	63.26
31.4				147.61	126.66				147.61	85.29				147.61	81.62
43.1				181.39	155.64				181.39	104.81				181.39	100.30
Reach 6															
Discharge (m^3/s)	D50	τ*c	τc	τo	τo / τc	D84	τ*c	τc	τo	τo / τc	D90	τ*c	τc	τo	τo / τc
4.2	1.3	0.045	0.95	34.88	36.84	2.9	0.045	1.31	34.88	26.73	3.5	0.045	1.41	34.88	24.79
8.5				62.11	65.60				62.11	47.59				62.11	44.14
14.2				85.87	90.68				85.87	65.79				85.87	61.02
21.7				106.88	112.87				106.88	81.88				106.88	75.95
31.4				125.58	132.62				125.58	96.21				125.58	89.24
43.1				148.12	156.42				148.12	113.48				148.12	105.26

Table 3.6 Shear Stress Calculations for Coarse Grain A-Axis

Shear Stress Calculations for Coarse Grain A-Axis (mm)															
Reach 1															
Discharge (m^3/s)	D50	τ^*_c	τ_c	τ_o	τ_o/τ_c	D84	τ^*_c	τ_c	τ_o	τ_o/τ_c	D90	τ^*_c	τ_c	τ_o	τ_o/τ_c
4.2	924	0.045	673.03	81.73	0.12	1389	0.045	792.23	81.73	0.10	1490	0.045	814.79	81.73	0.10
8.5				74.48	0.11				74.48	0.09				74.48	0.09
14.2				101.39	0.15				101.39	0.13				101.39	0.12
21.7				129.77	0.19				129.77	0.16				129.77	0.16
31.4				152.99	0.23				152.99	0.19				152.99	0.19
43.1				179.69	0.27				179.69	0.23				179.69	0.22
Reach 2															
Discharge (m^3/s)	D50	τ^*_c	τ_c	τ_o	τ_o/τ_c	D84	τ^*_c	τ_c	τ_o	τ_o/τ_c	D90	τ^*_c	τ_c	τ_o	τ_o/τ_c
4.2	641	0.045	466.90	115.41	0.25	920	0.045	539.50	115.41	0.21	981	0.045	553.54	115.41	0.21
8.5				142.75	0.31				142.75	0.26				142.75	0.26
14.2				175.61	0.38				175.61	0.33				175.61	0.32
21.7				206.87	0.44				206.87	0.38				206.87	0.37
31.4				237.21	0.51				237.21	0.44				237.21	0.43
43.1				266.30	0.57				266.30	0.49				266.30	0.48
Reach 3															
Discharge (m^3/s)	D50	τ^*_c	τ_c	τ_o	τ_o/τ_c	D84	τ^*_c	τ_c	τ_o	τ_o/τ_c	D90	τ^*_c	τ_c	τ_o	τ_o/τ_c
4.2	648	0.045	472.00	108.95	0.23	987	0.045	558.52	108.95	0.20	1180	0.045	599.88	108.95	0.18
8.5				140.61	0.30				140.61	0.25				140.61	0.23
14.2				172.54	0.37				172.54	0.31				172.54	0.29
21.7				204.87	0.43				204.87	0.37				204.87	0.34
31.4				236.41	0.50				236.41	0.42				236.41	0.39
43.1				266.80	0.57				266.80	0.48				266.80	0.44
Reach 4															
Discharge (m^3/s)	D50	τ^*_c	τ_c	τ_o	τ_o/τ_c	D84	τ^*_c	τ_c	τ_o	τ_o/τ_c	D90	τ^*_c	τ_c	τ_o	τ_o/τ_c
4.2	562	0.045	409.36	134.46	0.33	884	0.045	490.67	134.46	0.27	958	0.045	506.70	134.46	0.27
8.5				149.95	0.37				149.95	0.31				149.95	0.30
14.2				178.77	0.44				178.77	0.36				178.77	0.35
21.7				204.75	0.50				204.75	0.42				204.75	0.40
31.4				237.94	0.58				237.94	0.48				237.94	0.47
43.1				272.30	0.67				272.30	0.55				272.30	0.54
Reach 5															
Discharge (m^3/s)	D50	τ^*_c	τ_c	τ_o	τ_o/τ_c	D84	τ^*_c	τ_c	τ_o	τ_o/τ_c	D90	τ^*_c	τ_c	τ_o	τ_o/τ_c
4.2	676	0.045	492.39	49.19	0.10	1072	0.045	592.12	49.19	0.08	1415	0.045	661.66	49.19	0.07
8.5				62.11	0.13				62.11	0.10				62.11	0.09
14.2				82.70	0.17				82.70	0.14				82.70	0.12
21.7				114.42	0.23				114.42	0.19				114.42	0.17
31.4				147.61	0.30				147.61	0.25				147.61	0.22
43.1				181.39	0.37				181.39	0.31				181.39	0.27
Reach 6															
Discharge (m^3/s)	D50	τ^*_c	τ_c	τ_o	τ_o/τ_c	D84	τ^*_c	τ_c	τ_o	τ_o/τ_c	D90	τ^*_c	τ_c	τ_o	τ_o/τ_c
4.2	461	0.045	335.79	34.88	0.10	824	0.045	423.60	34.88	0.08	927	0.045	444.04	34.88	0.08
8.5				62.11	0.18				62.11	0.15				62.11	0.14
14.2				85.87	0.26				85.87	0.20				85.87	0.19
21.7				106.88	0.32				106.88	0.25				106.88	0.24
31.4				125.58	0.37				125.58	0.30				125.58	0.28
43.1				148.12	0.44				148.12	0.35				148.12	0.33

Table 3.7 Shear Stress Calculations for Coarse Grain B-Axis

Shear Stress Calculations for Coarse Grain B-Axis (mm)															
Reach 1															
Discharge (m^3/s)	D50	τ^*_c	τ_c	τ_o	τ_o/τ_c	D84	τ^*_c	τ_c	τ_o	τ_o/τ_c	D90	τ^*_c	τ_c	τ_o	τ_o/τ_c
4.2	353	0.045	257.12	81.73	0.32	545	0.045	305.91	81.73	0.27	599	0.045	317.69	81.73	0.26
8.5				74.48	0.29				74.48	0.24				74.48	0.23
14.2				101.39	0.39				101.39	0.33				101.39	0.32
21.7				129.77	0.50				129.77	0.42				129.77	0.41
31.4				152.99	0.60				152.99	0.50				152.99	0.48
43.1				179.69	0.70				179.69	0.59				179.69	0.57
Reach 2															
Discharge (m^3/s)	D50	τ^*_c	τ_c	τ_o	τ_o/τ_c	D84	τ^*_c	τ_c	τ_o	τ_o/τ_c	D90	τ^*_c	τ_c	τ_o	τ_o/τ_c
4.2	298	0.045	217.06	115.41	0.53	457	0.045	257.55	115.41	0.45	493	0.045	265.48	115.41	0.43
8.5				142.75	0.66				142.75	0.55				142.75	0.54
14.2				175.61	0.81				175.61	0.68				175.61	0.66
21.7				206.87	0.95				206.87	0.80				206.87	0.78
31.4				237.21	1.09				237.21	0.92				237.21	0.89
43.1				266.30	1.23				266.30	1.03				266.30	1.00
Reach 3															
Discharge (m^3/s)	D50	τ^*_c	τ_c	τ_o	τ_o/τ_c	D84	τ^*_c	τ_c	τ_o	τ_o/τ_c	D90	τ^*_c	τ_c	τ_o	τ_o/τ_c
4.2	273	0.045	198.85	108.95	0.55	431	0.045	238.70	108.95	0.46	466	0.045	246.27	108.95	0.44
8.5				140.61	0.71				140.61	0.59				140.61	0.57
14.2				172.54	0.87				172.54	0.72				172.54	0.70
21.7				204.87	1.03				204.87	0.86				204.87	0.83
31.4				236.41	1.19				236.41	0.99				236.41	0.96
43.1				266.80	1.34				266.80	1.12				266.80	1.08
Reach 4															
Discharge (m^3/s)	D50	τ^*_c	τ_c	τ_o	τ_o/τ_c	D84	τ^*_c	τ_c	τ_o	τ_o/τ_c	D90	τ^*_c	τ_c	τ_o	τ_o/τ_c
4.2	252	0.045	183.55	134.46	0.73	475	0.045	236.53	134.46	0.57	551	0.045	251.00	134.46	0.54
8.5				149.95	0.82				149.95	0.63				149.95	0.60
14.2				178.77	0.97				178.77	0.76				178.77	0.71
21.7				204.75	1.12				204.75	0.87				204.75	0.82
31.4				237.94	1.30				237.94	1.01				237.94	0.95
43.1				272.30	1.48				272.30	1.15				272.30	1.08
Reach 5															
Discharge (m^3/s)	D50	τ^*_c	τ_c	τ_o	τ_o/τ_c	D84	τ^*_c	τ_c	τ_o	τ_o/τ_c	D90	τ^*_c	τ_c	τ_o	τ_o/τ_c
4.2	326	0.045	237.46	49.19	0.21	474	0.045	275.81	49.19	0.18	506	0.045	283.11	49.19	0.17
8.5				62.11	0.26				62.11	0.23				62.11	0.22
14.2				82.70	0.35				82.70	0.30				82.70	0.29
21.7				114.42	0.48				114.42	0.41				114.42	0.40
31.4				147.61	0.62				147.61	0.54				147.61	0.52
43.1				181.39	0.76				181.39	0.66				181.39	0.64
Reach 6															
Discharge (m^3/s)	D50	τ^*_c	τ_c	τ_o	τ_o/τ_c	D84	τ^*_c	τ_c	τ_o	τ_o/τ_c	D90	τ^*_c	τ_c	τ_o	τ_o/τ_c
4.2	256	0.045	186.47	34.88	0.19	423	0.045	237.36	34.88	0.15	462	0.045	236.14	34.88	0.15
8.5				62.11	0.33				62.11	0.26				62.11	0.26
14.2				85.87	0.46				85.87	0.36				85.87	0.36
21.7				106.88	0.57				106.88	0.45				106.88	0.45
31.4				125.58	0.67				125.58	0.53				125.58	0.53
43.1				148.12	0.79				148.12	0.62				148.12	0.63

Table 3.8 Shear Stress Calculations for Coarse Grain C-Axis

Shear Stress Calculations for Coarse Grain C-Axis (mm)															
Reach 1															
Discharge (m^3/s)	D50	τ^*_c	τ_c	τ_o	τ_o/τ_c	D84	τ^*_c	τ_c	τ_o	τ_o/τ_c	D90	τ^*_c	τ_c	τ_o	τ_o/τ_c
4.2	106	0.045	77.21	81.73	1.06	242	0.045	107.42	81.73	0.76	329	0.045	121.46	81.73	0.67
8.5				74.48	0.96				74.48	0.69				74.48	0.61
14.2				101.39	1.31				101.39	0.94				101.39	0.83
21.7				129.77	1.68				129.77	1.21				129.77	1.07
31.4				152.99	1.98				152.99	1.42				152.99	1.26
43.1				179.69	2.33				179.69	1.67				179.69	1.48
Reach 2															
Discharge (m^3/s)	D50	τ^*_c	τ_c	τ_o	τ_o/τ_c	D84	τ^*_c	τ_c	τ_o	τ_o/τ_c	D90	τ^*_c	τ_c	τ_o	τ_o/τ_c
4.2	89	0.045	64.83	115.41	1.78	178	0.045	85.54	115.41	1.35	221	0.045	93.27	115.41	1.24
8.5				142.75	2.20				142.75	1.67				142.75	1.53
14.2				175.61	2.71				175.61	2.05				175.61	1.88
21.7				206.87	3.19				206.87	2.42				206.87	2.22
31.4				237.21	3.66				237.21	2.77				237.21	2.54
43.1				266.30	4.11				266.30	3.11				266.30	2.86
Reach 3															
Discharge (m^3/s)	D50	τ^*_c	τ_c	τ_o	τ_o/τ_c	D84	τ^*_c	τ_c	τ_o	τ_o/τ_c	D90	τ^*_c	τ_c	τ_o	τ_o/τ_c
4.2	76	0.045	55.36	108.95	1.97	136	0.045	69.87	108.95	1.56	192	0.045	69.87	108.95	1.56
8.5				140.61	2.54				140.61	2.01				140.61	2.01
14.2				172.54	3.12				172.54	2.47				172.54	2.47
21.7				204.87	3.70				204.87	2.93				204.87	2.93
31.4				236.41	4.27				236.41	3.38				236.41	3.38
43.1				266.80	4.82				266.80	3.82				266.80	3.82
Reach 4															
Discharge (m^3/s)	D50	τ^*_c	τ_c	τ_o	τ_o/τ_c	D84	τ^*_c	τ_c	τ_o	τ_o/τ_c	D90	τ^*_c	τ_c	τ_o	τ_o/τ_c
4.2	76	0.045	55.36	134.46	2.43	154	0.045	41.79	134.46	3.22	203	0.045	73.43	134.46	1.83
8.5				149.95	2.71				149.95	3.59				149.95	2.04
14.2				178.77	3.23				178.77	4.28				178.77	2.43
21.7				204.75	3.70				204.75	4.90				204.75	2.79
31.4				237.94	4.30				237.94	5.69				237.94	3.24
43.1				272.30	4.92				272.30	6.52				272.30	3.71
Reach 5															
Discharge (m^3/s)	D50	τ^*_c	τ_c	τ_o	τ_o/τ_c	D84	τ^*_c	τ_c	τ_o	τ_o/τ_c	D90	τ^*_c	τ_c	τ_o	τ_o/τ_c
4.2	76	0.045	55.36	49.19	0.89	166	0.045	75.67	49.19	0.65	197	0.045	75.67	49.19	0.65
8.5				62.11	1.12				62.11	0.82				62.11	0.82
14.2				82.70	1.49				82.70	1.09				82.70	1.09
21.7				114.42	2.07				114.42	1.51				114.42	1.51
31.4				147.61	2.67				147.61	1.95				147.61	1.95
43.1				181.39	3.28				181.39	2.40				181.39	2.40
Reach 6															
Discharge (m^3/s)	D50	τ^*_c	τ_c	τ_o	τ_o/τ_c	D84	τ^*_c	τ_c	τ_o	τ_o/τ_c	D90	τ^*_c	τ_c	τ_o	τ_o/τ_c
4.2	74	0.045	53.90	34.88	0.65	146	0.045	70.74	34.88	0.49	189	0.045	78.43	34.88	0.44
8.5				62.11	1.15				62.11	0.88				62.11	0.79
14.2				85.87	1.59				85.87	1.21				85.87	1.09
21.7				106.88	1.98				106.88	1.51				106.88	1.36
31.4				125.58	2.33				125.58	1.78				125.58	1.60
43.1				148.12	2.75				148.12	2.09				148.12	1.89

3.6 Comparison of Competency Results

This research utilizes two methods to determine the largest grain size mobilized, and two methods to determine discharges in Cheaha Creek. The original Costa Method uses the particle diameter to predict velocity and average depth of flow. This thesis research rearranges the original Costa Equation (Figure 2.1) to predict a mobile grain size from known values of mean depth (Equation 2.2), and velocity is then computed using Costa's original Velocity Equation (Equation 2.1) The Adjusted Shields Equation calculates the tractive force applied on an object by the surrounding fluid (τ_o), and compares that value to the resistance of a sediment grain to the applied force. The Costa Method produces competent grain size values nearly an order of magnitude greater than the Adjusted Shields Equation at discharges less than 10 m^3/s (353 cfs). This large difference is likely attributed to the local differences in hydraulics at lower discharges between the streams from which Costa (1983) compiled his data and the Cheaha Creek study section. Figure 3.16 shows the relationship between discharge and competent particle size for both methods, and Table 3.7 shows the percent differences in competent particle sizes between both methods. Differences become smaller at larger discharges, but remain close to 100 percent.

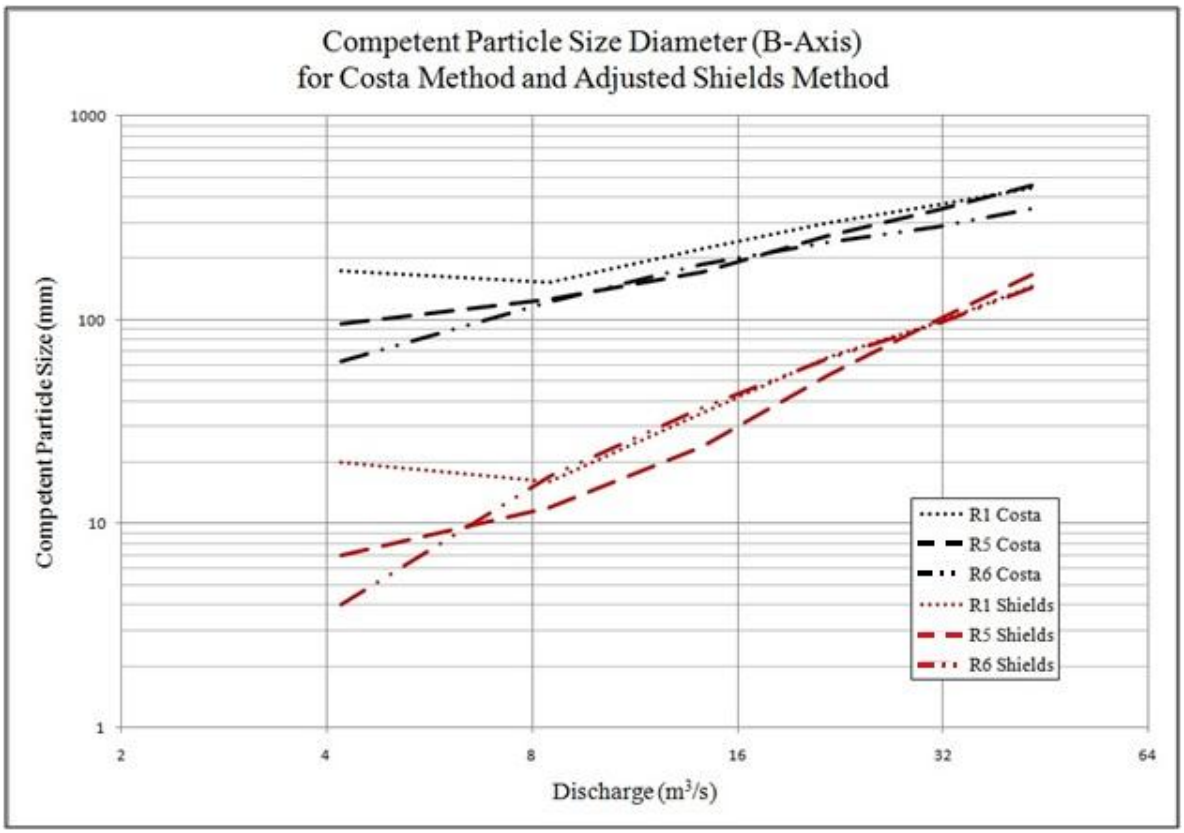

Figure 3.16 Comparison of competent particle sizes using the Costa Method and the Adjusted Shields Method for Study Reaches 1, 5, and 6

Table 3.9 Differences in calculated competent particle sizes between the Costa Method and the Adjusted Shields Method in Study Reaches 1, 5, and 6.

Difference in Competent Particle Size B-Axis (mm) in the Costa Method and the Adjusted Shields Method									
	Reach 1			Reach 5			Reach 6		
Discharge (m^3/s)	Shields	Costa	% Difference	Shields	Costa	% Difference	Shields	Costa	% Difference
4.2	20	174	159	7	95	173	4	62	176
8.5	16	152	162	12	126	165	17	123	151
14.2	35	222	146	24	172	151	37	186	134
21.7	65	297	128	53	257	132	64	239	116
31.4	97	365	116	100	348	111	96	288	100
43.1	145	445	102	167	456	93	144	349	83

3.7 Flow Frequency Analysis

A flow frequency relationship must be determined in order for assumptions to be made regarding the frequency of coarse grain sediment transport. Because Cheaha Creek is an ungaged stream, estimations of the frequency of discharge values are calculated using regression equations developed for small rural streams in Alabama (Hedgecock, 2004). These equations are based on peak discharge data at 43 USGS gaging stations on small basin rural streams in Alabama and adjacent states, each with 10 or more years of discharge record. The dependent variable in these equations is drainage area, which was shown to be the most significant variable in the prediction of discharge (Hedgecock, 2004). Other variables tested by Hedgecock were average channel slope, channel length, a basin lag-time factor, drainage area percent forest cover, and drainage basin width to length ratio. Table 3.8 adapted from Hedgecock (2004) shows the accuracy of the flood frequency regression equations. Equivalent years of peak flow record in column 3 refer to the number of years of recorded peak flow data required to provide an estimate of flood frequency equal to the regression estimation.

Table 3.10 Accuracy of flood frequency relations for small rural streams in Alabama.

Accuracy of Flood Frequency Equations (from Hedgecock, 2004)		
Recurrence Interval (years)	Standard Error of Prediction (percent)	Equivalent Years of Peak Flow Record
2	53	2
5	35	5
10	30	9
25	29	13
50	31	14
100	35	14
200	40	13
500	47	12

Flow frequency values in Cheaha Creek are derived from slope-area calculations of discharges as well as regression equations developed by Hedgecock (2004). The regression equations were used to determine discharges in Cheaha Creek with recurrence intervals of 2, 5, 10, 25, 50, 100, 200, and 500 years. The slope-area discharges calculated in this thesis research were then fit to the computed regression curve (Figure 3.17).

The flow frequency values for slope-area discharges computed for Cheaha Creek are as follows: 6 day flow (4.2 m^3/s), 43 day flow (8.5 m^3/s), 1.5 year flow (14.2 m^3/s), 2 year flow (21.7 m^3/s), 4.5 year flow (31.4 m^3/s), and the 8.5 year flow (43.1 m^3/s). The 1.5 and 2 year recurrence intervals typically represent bankfull discharge in alluvial channels, (Leopold *et al.*, 1964). Interestingly, the 1.5 year flow in Cheaha Creek corresponds with bankfull elevation in both of the slope-area cross-sections as well as the Reach 5 cross-section. This finding provides a "ground-truth" of sorts for these flow frequency data because the discharges as well as the recurrence intervals computed in this thesis research are based solely on equations and modeling using hydraulic principles, rather than field measurements.

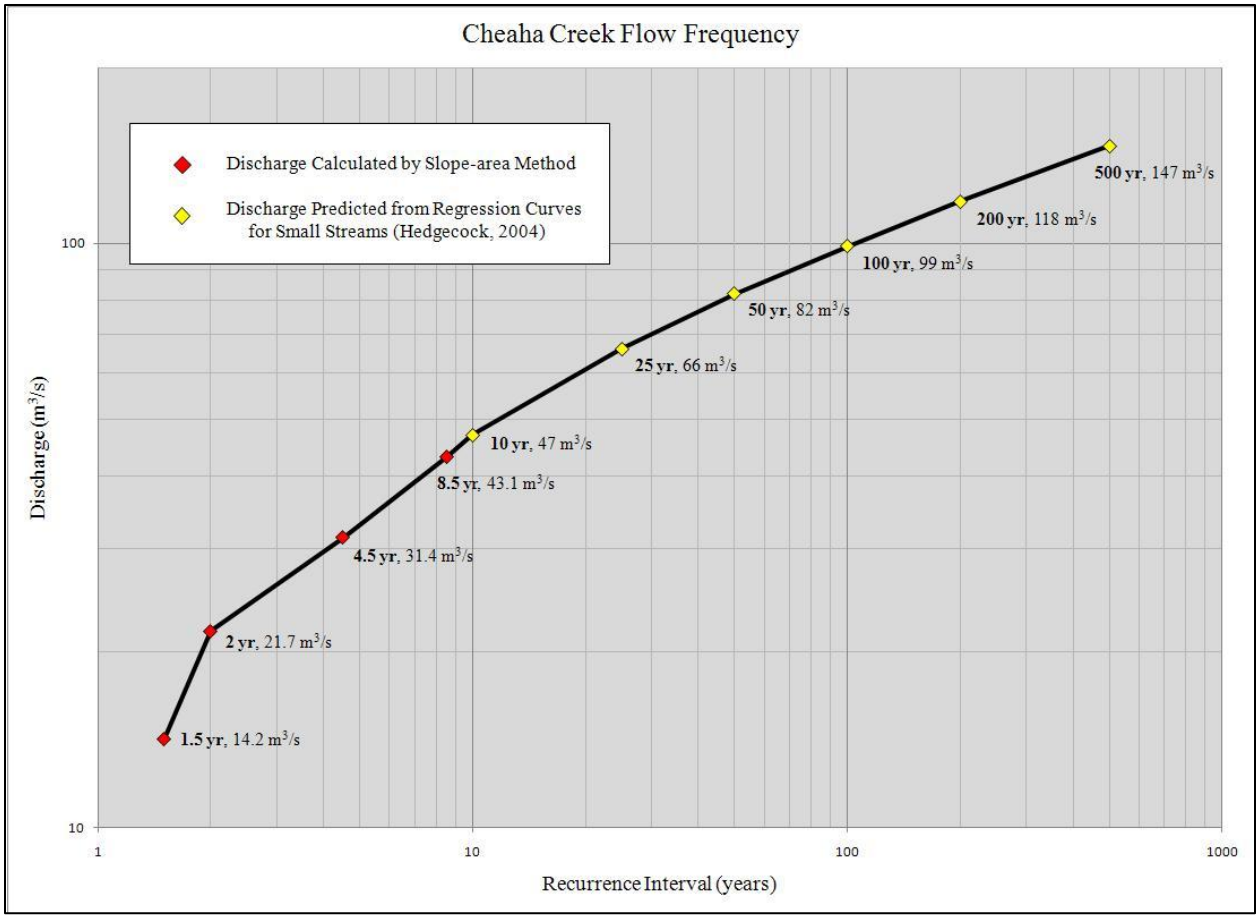

Figure 3.17 Flow frequency for Cheaha Creek calculated from the Slope-Area Equation and regression equations for small rural streams (Hedgecock, 2004).

CHAPTER 4

4.0 DISCUSSION

This chapter explores the results from hydraulic calculations of discharge as well as discrepancies between the Costa Method and the Adjusted Shields Method for determining competent particle size. Interpretation of sediment transport findings related to landscape evolution in the Talladega Mountains is also presented.

4.1 Discharge Calculations

The Slope-Area Equation and the Costa Method to compute discharge are compared in this research, and large differences in flow values are observed. Discharges are calculated using the Costa method for all cross-sections surveyed in Cheaha Creek, but the only values used for this comparison were from the two slope-area cross-sections (Figure 2.2). The Slope-Area Equation was used throughout this thesis research to estimate discharge because it utilizes a more empirical and precise approach to computing flow. Compared to the Slope-Area Equation the Costa Method overestimated discharges in the upstream slope-area cross-section, typically by a factor of 3 at each gage height. This was due to much greater predictions of velocity in the Costa method. The downstream slope-area cross-section showed much less variability in velocities and resulting discharges, with differences in the latter ranging from 20 - 50 percent. Discharge values

computed with the Slope-Area Equation can exhibit variability depending on the roughness values that are given to a particular reach or sub-section. Predictions of discharge in the downstream slope-area cross-section may have shown better agreement between methods if roughness values were reduced, however this would not be an accurate representation of reach characteristics in Cheaha Creek. The most accurate way to determine the actual roughness values in Cheaha Creek would be to make a discharge measurement at a level of flow that included at least some part of each roughness subsection (i.e. channel, left overbank, right overbank) (Figure 2.2). The actual roughness values could then be computed by rearranging the Manning Equation (Equation 2.7) to solve for *n*. Overall the Costa Method provides a decent estimation of discharge for paleohydraulic reconstruction applications. However, results from this research indicate that apart from an actual discharge measurement, the Slope-Area Equation should be used when field data such as the slope of the water surface, cross-sectional area, and roughness values are able to be determined.

4.2 Competent Particle Size

4.2.1 Water Surface Slope

Mean bed shear stress values used to compute competent particle sizes were overestimated in this thesis research for Study Reaches 2, 3, and 4. This overestimation of τ_o results from using the average Study Section slope (0.014) to represent the water surface profile. Figure 3.1 shows the longitudinal profile of the channel bed and assumed water surface, along with an estimate of a more likely water surface profile. Using the average bed slope of the channel bed is better suited for streams with low gradients and gradual breaks in slope. Steep mountain streams like Cheaha Creek exhibit sharper breaks in slope, and these abrupt changes

increase the likelihood of transcritical flow. The transition from subcritical flow (Froude ≤ 1) to supercritical flow (Froude ≥ 1) typically results in the formation of hydraulic jumps. The depth of flow is usually more shallow where supercritical flow occurs and deeper in subcritical conditions. The more likely water surface profile in Figure 3.1 roughly accounts for the depth changes in areas where hydraulic jumps may exist. This profile is merely an educated guess based on previous experience and is used for qualitative purposes only.

Another problem that arises when using the average bed slope for the Study Section of Cheaha Creek is the overestimation of depth at the reaches where the bed exhibits a more concave upward shape (river station 25 - 225). This apparent increase in depth is misleading, especially when calculating mean bed shear stress at these reaches. This increase in depth is especially evident when comparing the cross-sectional area, wetted perimeter, and resulting hydraulic radius for the study reaches (Table 3.1, p 50). Cross-sections for reaches 2, 3, and 4 are located within this zone of depth overestimation, and the cross-sectional area at a GH = 1.2 for these three reaches ranges from 17.65 - 19.69 m^2. The cross-sectional area for reaches 1, 5, and 6 at the same gage height (GH=1.2) ranges from 1.86 - 7.62 m^2. This difference however does not signify that any computations were incorrect, only that the water surface elevations at which the hydraulic properties were computed do not correctly correspond with the slope-area discharge's water surface. For this thesis research, the most accurate hydraulic properties and resulting mean bed shear stress values used are for Study Reach 1, Study Reach 5, and Study Reach 6 due to the more realistic depths when using the average bed slope as the water surface profile.

4.2.2 Coarse Grain Transport

The Critical Shear Stress Equation (Equation 2.6) is used to determine the coarse grain sizes that exhibit a ratio of τ_o / τ_c equal to, or slightly greater than 1.0. For this thesis research, it is assumed that when the ratio of $\tau_o / \tau_c \geq 1.0$, the grain size to which bed stress is applied should experience motion. However, this grain size may not actually be mobile at the calculated discharge depending on local hydraulic conditions. These results are based on the assumption that local hydraulics are equal across and throughout each study reach. As stated earlier, Equation 2.6 calculates τ_c with regard to the D_{50} size of the surrounding grains. This thesis research calculates τ_c for coarse grains using the D_{50} of each of the *a*, *b*, and *c-axis* grain size populations. The *b-axis* is typically used to describe the size of a sediment grain, and thus the surrounding population of grains. However, due to the poor sorting of sizes and heterogeneity of grain pocket geometry, the *b-axis* alone does not always provide the best description of a coarse sediment grain in Cheaha Creek. A sediment grain resting on the channel bed may be sheltered from flow by the length of any axis of the surrounding particles. This thesis research addresses this issue by using each axis D_{50} in the τ_c computations in order to present a range of the largest possibly mobile grain sizes. Each competent grain size shown for each axis in Table 4.1 is calculated based on the assumption that the grain is sheltered by only the lengths of each particular axis. For example, in Study Reach 1 at a discharge of 4.2 m^3/s, if all of the surrounding grains were situated where the *a-axis* was the length that sheltered a grain from flow, the largest mobile clast would be 5 mm. If the *c-axis* was the sheltering length for the same reach and flow, the largest mobile clast would be 123 mm. This range of competent grain sizes is shown in Table 4.1 only for Study Reaches 1, 5, and 6 due to the overestimation of τ_o in Study Reaches 2, 3, and 4. Competent grain sizes computed with this method cover a very broad spectrum, and

encompass nearly the entire range of grain sizes found in Cheaha Creek. For the largest calculated discharge of 43.1 m^3/s (1524 cfs), it is estimated that the largest mobile particle ranges from 34 -878 mm in Study Reach 1, 55 - 1480 mm in Study Reach 5, and 59 - 927 mm in Study Reach 6. These results infer that if perfectly situated, nearly all coarse sediment clasts are potentially mobile in Cheaha Creek at the calculated discharge of 43.1 m^3/s (1524 cfs). Clasts are not always, if ever, situated in the optimal position for movement, especially in tightly packed alluvial steps, but based on these results it can be concluded that Cheaha Creek is capable of moving these particles in the current climatic regime.

Table 4.1 Competent grain sizes calculated from the grain size distribution of each axis diameter.

Competent Grain Size Diameter (mm) Calculated with Respect to the Grain Size Distribution of each Axis (where $\tau_o / \tau_c \geq 1$)			
A-Axis Grain Size Distribution			
Discharge (m^3/s)	Reach 1	Reach 5	Reach 6
4.2	5	2	1
8.5	3	3	6
14.2	8	7	15
21.7	16	17	26
31.4	22	33	39
43.1	34	55	59
B-Axis Grain Size Distribution			
Discharge (m^3/s)	Reach 1	Reach 5	Reach 6
4.2	20	7	4
8.5	16	12	17
14.2	35	24	37
21.7	65	53	64
31.4	97	100	96
43.1	145	167	144
C-Axis Grain Size Distribution			
Discharge (m^3/s)	Reach 1	Reach 5	Reach 6
4.2	123	57	25
8.5	97	102	106
14.2	210	208	238
21.7	389	467	410
31.4	586	883	614
43.1	876	1480	927

4.2.3 Fine Grain Transport

Results shown in Table 3.5 indicate that the sediments which compose the fine grain distinct deposits are frequently mobilized, even at lower discharges. It may also be inferred from these findings that much of the abrasive wear seen throughout Cheaha Creek, in the form of both potholes and depressions on the crests of bedrock outcrops, is likely due to the high frequency of movement of this finer grain sediment population. Equation 2.6 calculates τ_c with regard to the D_{50} grain size of the surrounding grains, and for the fine grain sample the D_{50b} of the distinct deposits is used. Interestingly, if τ_c is calculated using the D_{50b} of the coarse grain sample instead, τ_o / τ_c ratios range from 1.04 - 6.57 in all study reaches. This observation shows that these finer grains likely remain mobile, even when partially sheltered due to the greater size of the surrounding coarse population.

4.3 Topographic Evolution of the Talladega Mountains

This thesis research provides useful data regarding sediment transport processes and the resulting denudation of the Talladega Mountains of Northeastern Alabama. The frequency of mobilization of coarse sediments as well as step-pool and cascade bedforms as a whole plays an important role in the denudation of post-orogenic mountain environments. Headwater mountain streams typically control the rates of topographic decay in non-glaciated mountain environments (Whipple, 2004). In mixed bedrock-alluvial streams such as Cheaha Creek, erosion of the channel bed occurs both when grains are entrained in flow and abrade the bed and when blocks of bedrock are loosened and finally plucked from the bed. Evidence of both processes is visible in the Study Section of Cheaha Creek.

Results from this thesis research suggest that bedrock erosion can occur on relatively short time scales in Cheaha Creek. Depending on the sheltering axis, coarse gravel to large cobbles are potentially mobile at 1.5 year recurrence interval flows, and the 4.5 - 8.5 year flows can potentially mobilize small to large boulders. Results also indicate that a range of particle sizes are potentially mobile across a range of flows. As clasts are moved and situated in different positions, other clasts that were once sheltered from flow become exposed and their mobility is increased. This implies that Cheaha Creek is quite efficient in moving sediment grains downstream. Perhaps even more significant, fine-grain deposits are typically mobile even at the lowest calculated discharge, which represents the one week recurrence interval flow. Because fine grain particles are so frequently mobile, even a small amount of erosion is likely to occur after even short lived storm events that only minimally increase discharge.

It should also be noted that some coarse grain clasts were partially to nearly fully embedded in the channel margins. This may be evidence of a recent or ongoing accretion event in the Study Section. The channel is horizontally confined to a straight reach in this section due to relatively narrow valley walls, so it is unlikely that the embedded clasts are remnants of a former channel meander. This is an important observation because it may be evidence of accretionary fill from heavy logging that occurred in the upper drainage basin within the last 150 years. If the majority of this fine grain sediment has been recently introduced, it could signify that the stream is currently adjusting and the fine grain sediment currently found in the channel may not have been continuously present over geologic history. Implications for landscape evolution from this hypothesis could signify that the current channel dimensions and thus shear stress values may be an underestimate of the channel characteristics over geologic time. However because the valley slopes are so tightly coupled in the Study Section the embedded

clasts may have been covered instead by a mass movement event, although no evidence of such event, at least in recent history, was readily visible.

Because Cheaha Creek exhibits primarily supply-limited characteristics, sediment input rates essentially limit erosion and the resulting landscape evolution in this drainage basin (Whipple and Tucker, 2002). For erosion to occur, the alluvial cover must be mobilized and induce abrasive wear on the bedrock streambed. In a humid environment such as the Talladega Mountains where annual rainfall totals can exceed 140 cm, bedrock erosion rates may be relatively fast compared to other post-orogenic landscapes. However rates of bedrock erosion would typically be much less when compared to active orogens with similar climates and greater sediment supply such as the Cascade Range in the Pacific Northwest.

This thesis shows that sediment mobilizing discharges occur on relatively short timescales in Cheaha Creek, thus initiating erosion and lowering the base level of the landscape. Future research to observe coarse grain particle movement after floods, measuring discharge during floods, and monitoring bedrock erosion with developing technologies such as terrestrial light detection and ranging (T-LIDAR) would provide more data and insight into the problem of landscape evolution in the Talladega Range.

REFERENCES

Abbe, T., and D. Montgomery. 1996. Interaction of large woody debris, channel hydraulics and habitat formation in large rivers. Regulated Rivers: Research and Management. 12. 201-221

Andrews, E. 1983. Entrainment of gravel from naturally sorted riverbed material. Geological Society of America Bulletin. 94. 1225-1231

Arcement, G. and V. Schneider. 1989. Guide for selecting Manning's roughness coefficients for natural channels and floodplains. pp 11 U.S. Geological Survey Water Supply Paper 2339.

Barnes, H. 1967. Roughness characteristics of natural channels. U.S. Geological Survey Water Supply Paper 1849.

Bathurst, J.C. 1987. Flow resistance in boulder-bed streams. In: Hey, R.D., Bathurst, J.C., Thorne, C.R. (Eds.). Gravel-Bed Rivers. Wiley. Chichester, UK. 403– 465.

Bilby, R., and G. Likens. 1980. Importance of organic debris dams in the structure and function of stream ecosystems. Ecology. 61. 1107-1113

Bisson, P. and eight co-authors. 1987. Large woody debris in forested streams in the Pacific Northwest: past, present, and future. pp. 143-190 in E. Salo and T. Cundy (Eds.) Streamside Management: Forestry and Fishery Interactions. University of Washington, Seattle.

Bradley, W. and A. Mears. 1980. Calculations of flows needed to transport coarse fraction of Boulder Creek alluvium at Boulder, Colorado. Geological Society of America Bulletin. II. 91. 1057-1090

Buffington, J. 1999. The legend of A.F. Shields. Journal of Hydraulic Engineering. 125. 4. 376-387

Buffington, J. and Montgomery, D. 1997. A systematic analysis of eight decades of incipient motion studies with special reference to gravel bedded rivers. Water Resources Research. 33. 8. 1993-2029

Costa, J. 1983. Paleohydraulic reconstruction of flashflood peaks from boulder deposits in the Colorado Front Range. Geological Society of America Bulletin. 94. 986-1004

Cowen, W. 1956. Estimating hydraulic roughness coefficients. Agricultural Engineering. 37. 7. 473-475

Charlton, R. 2008. Fundamentals of Fluvial Geomorphology. Routledge. New York

Chin, A. 1989. Step-pools in stream channels. Progress in Physical Geography. 13. 391-408

Chin, A. 1998. On the stability of step-pool streams. The Journal of Geology. 106. 59-69

Chin, A. 1999. The morphologic structure of step-pools in mountain streams. Geomorphology. 27. 191-204

Chin, A. 2002. The periodic nature of step-pool mountain streams. American Journal of Science. 302. 144-167

Chin, A. 2003. The geomorphic significance of step-pools in mountain streams. Geomorphology. 55. 125-137

Chin, A., and E. Wohl. 2005. Toward a theory for step-pools in stream channels. Progress in Physical Geography. 3. 275-296

Dalrymple, T., and Benson, M. 1967. Measurement of peak discharge by the slope-area method: U.S. Geological Survey Techniques of Water-Resources Investigations. Book 3. A2. 12

Dolloff, C. 1986. Effects of stream cleaning on juvenile Coho salmon and Dolly varden in southeast Alaska. Transactions of the American Fisheries Society. 115. 743-755

Duckson, D., and L. Duckson. 2001. Channel bed steps and pool shapes along Soda Creek, Three Sisters Wilderness, Oregon. Geomorphology. 38. 267-279

Dunne, T., W. Zhang, B. Aubry. 1991. Effects of Rainfall, Vegetation, and Microtopography on Infiltration and Runoff. Water Resources Research. 27. 9. 2271-2285

Franklin, J. 1982. Ecosystem studies in the Hoh River drainage, Olympic National Park. In: Starkey, Franklin, and Matthews (Eds.) Ecological Research in National Parks of the Pacific Northwest

Grant, G., F. Swanson, G. Wolman. 1990. Pattern and origin of stepped-bed morphology in high gradient streams, Western Cascades, Oregon. Geological Society of America Bulletin. 102. 340-352

Gregory, K., and R. Davis. 1992. Coarse woody debris in stream channels in relation to river channel management in woodland areas. Regulated Rivers: Resource and Management. 7. 117-136

Harmon, M., J. Franklin, F. Swanson. 1986. Ecology of coarse woody debris in temperate ecosystems. Advanced Ecological Research. 11. 436-444

Hedgecock, T. 2004. Magnitude and frequency of floods on small rural streams in Alabama. U.S. Geological Survey Scientific Investigations Report. 2004-5135

Hjulstrom, F. 1935. Studies of the morphological activities of rivers as exhibited by the River Fyris: Uppsala, Sweden. University of Uppsala Geology Bulletin. 25. 221-527

Jackson W., and R. Beschta. 1982. A model of two-phase bedload transport in an Oregon coast range stream. Earth Surface Processes and Landforms. 7. 517-527

Jansen, J. 2006. Flood magnitude–frequency and lithologic control on bedrock river incision in post-orogenic terrain. Geomorphology. 82. 39-57

Keller, E., and W. Melhorn. 1978. Rhythmic spacing and origin of pools and riffles. Geological Society of America Bulletin. 89. 723-730

Komar, P. 1987. Selective gravel entrainment and the empirical evaluation of flow competence. Sedimentology. 34. 6. 1165-1176

Köppen, W. 1900. Versuch einer Klassifikation der Klimate, vorzugsweise nach ihren Beziehungen zur Pflanzenwelt.– Geogr. Zeitschr. 6. 593–611. 657–679

Leopold, L., G. Wolman, J. Miller. 1964. Fluvial Processes in Geomorphology. Dover Publications. New York

Leliavsky, S. 1955. An introduction to fluvial hydraulics. London. Constable. 257

Marston, R. 1982. The geomorphic significance of log steps in forested streams. Annals of the Association of American Geographers. 72. 99-108

Miller, M., I. McCave, P. Komar. 1977. Threshold of sediment motion under unidirectional currents. Sedimentology. 24. 507-527.

Montgomery, D., and J. Buffington. 1997. Channel reach morphology in mountain drainage basins. Geological Society of America Bulletin. 109. 5. 596-611

Montgomery, D., and K. Gran. 2001. Downstream variations in the width of bedrock channels. Water Resources Research. 37. 6. 1841-1846

Parker, G., and P. Klingeman. 1982. On why gravel bed streams are paved. Water Resources Research. 18. 1409-1423

Richards, K. 1976. The morphology of riffle pool sequences. Earth Surface Processes. 1. 71-88

Sedell, J., P. Bisson, F. Swanson, S. Gregory. 1988. Maser, Tarrant, Trappe, and Franklin (Eds.) From the Forest to the Sea: the Story of Fallen Trees. 153

Shields, A. 1936. Application of similarity principals and turbulence research to bedload movement. In Ott, W.P. and van Uchelen, J.C. (translators) California Institute of Technology. W.M. Keck Laboratory of Hydraulics and Water Resources, Report No. 167

Skylar, L., and W. Dietrich. 2006. The role of sediment in controlling steady-state bedrock channel slope: Implications of the saltation–abrasion incision model. Geomorphology. 82. 58-83

Southeastern Regional Climate Center. 2010. Station 018024. Talladega, AL. Monthly Climate Summary. http://www.sercc.com/cgi-bin/sercc/cliMAIN.pl?al8024. Last accessed 5/11/2010.

Szabo, M., E. Osborne, C. Copeland, T. Neathery. 1988. Geologic Map of Alabama. Geological Survey of Alabama Special Map 220. Scale 1:250,000

Thorne, C. and L. Zevenberger. 1986. Estimating mean velocity in mountain rivers. Journal of Hydraulic Engineering. 111. 612-624

Tomkin, J., M. Brandon, F. Pazzaglia, J. Barbour, S. Willett. 2003. Quantitative testing of bedrock incision models for the Clearwater River, NW Washington State. Journal of Geophysical Research. 108. B6

Wallace, J., J. Webster, J. Meyer. 1995. Influence of log additions on physical and biotic characteristics of a mountain stream. Canadian Journal of Fisheries and Aquatic Sciences. 52. 2120-2137

Whipple, K. 2004. Bedrock rivers and the geomorphology of active orogens. Annual Review of Earth and Planetary Science. 32. 151-189

Whipple, K., and G. Tucker. 2002. Implications of sediment flux-dependent river incision models for landscape evolution. Journal of Geophysical Research 107. B2

Whiting, S. 2009. Geology of the Talladega Slate Belt and the Foreland Fold-and-Thrust Belt, Talladega County, Alabama. Master's Thesis. The Florida State University Department of Geological Sciences.

Wiberg, P., and D. Smith. 1987. Calculations of the critical shear stress for motion of uniform and heterogeneous sediments. Water Resources Research. 23. 8. 1471-1480

Wolman, M. 1954. A method of sampling coarse river-bed material. Transactions of the American Geophysical Union. 35. 6. 951-956